Energy & Buildings 250 (2021) 111251

Contents lists available at ScienceDirect

Energy & Buildings

journal homepage: www.elsevier.com/locate/enb

Assessment of solar radiation data quality in typical meteorological years and its influence on the building performance simulation

Facundo Bre [a,*], Rayner M. e Silva Machado [b], Linda K. Lawrie [c], Drury B. Crawley [d], Roberto Lamberts [b]

[a] Centro de Investigación de Métodos Computacionales (CIMEC), UNL, CONICET, Predio "Dr. Alberto Cassano", Colectora Ruta Nacional 168, Paraje El Pozo, 3000, Santa Fe, Argentina
[b] Laboratory of Energy Efficiency in Buildings (LabEEE), Department of Civil Engineering, Federal University of Santa Catarina (UFSC), Florianópolis, Brazil
[c] DHL Consulting LLC, Pagosa Springs, CO, USA
[d] Bentley Systems, Inc., Washington, DC, USA

ARTICLE INFO

Article history:
Received 3 May 2021
Revised 19 June 2021
Accepted 1 July 2021
Available online 06 July 2021

Keywords:
Typical meteorological year
Solar radiation modeling
Validation
Building performance simulation
Building performance regulation
Tropical climate

ABSTRACT

Solar radiation along with other weather variables are commonly processed on typical meteorological years (TMYs) to be applied in the design of various energy systems. However, in several regions of the world, solar radiation data usually lacks a suitable and/or representative measurement, which leads to its modeling and prediction to properly fill this information in the databases. Consequently, the accuracy of these models can influence the viability and proper design of such energy systems. Within this context, the present contribution aims to assess the quality of solar radiation data included in the most recent TMY databases with Brazilian data and how that quality can influence the selection of months that create TMYs as well as the building performance simulation (BPS) results. Because two different approaches to generate the solar radiation data are used, we evaluate the global horizontal irradiation data in the two latest versions of recent Brazilian TMY databases against the corresponding satellite-derived ones obtained from the POWER database (NASA). Simultaneously, as another alternative approach, global solar radiation data are calculated for the same studied locations and period through the modeling method used to generate the current version of the International Weather for Energy Calculations (IWEC2), and its performance is also compared against the corresponding reanalysis data (POWER). Finally, a set of case studies applying the local building performance regulations are exhaustively analyzed to quantify the impact of the uncertainty of solar radiation models on BPS results throughout Brazil. The results indicate that the accuracy of solar radiation models can highly influence the resulting TMY configurations. These changes can drive differences up to 40% on the prediction of the ideal annual loads of the residential buildings while, regardless of design performance, differences lower than 10% are found for the commercial case studies in most locations. Conversely, the prediction of peak loads for cooling shows to be more sensitive to the climate data changes in the commercial buildings than in the residential ones.

Abbreviations: ABNT, Brazilian association of technical standards; AFN, Airflow network; BPS, Building performance simulation; BSRN, Baseline surface radiation network; Cp, Wind pressure coefficient; CRM, Cloudy-sky radiation model or Kasten's model; FARMS, Fast all-sky radiation model for solar applications; GHI, global horizontal irradiation; GHSR, Global Horizontal Solar Radiation; HVAC, Heating, Ventilation, and Air-Conditioning; $I_0 = 1367.7\ \mathrm{W/m^2}$, Solar constant; INMET, National institute of meteorology; IWEC, International weather for energy calculations; nDiff, Normalized difference error; nMSE, Normalized mean bias error; NOAA, National Oceanic and Atmospheric Administration; nRMSE, Normalized root mean square error; NSRDB, National solar radiation data base; PHWOT, Percentage of hours within the preset range of operative temperatures; PSM, Physical solar model; RH, Relative humidity; SA, Solar altitude; SHGC, Solar heat gain coefficient; SSE, Surface meteorology and solar energy project; TMM, Typical meteorological month; TMY, Typical meteorological year; TRY, Test reference year; TSC, Total sky cover; WMO, World meteorological organization; WWR, Window-to-wall ratio; WYEC, Weather year for energy calculations; ZHM, Zhang-Huang solar radiation model.

* Corresponding author.
E-mail address: facubre@cimec.santafe-conicet.gov.ar (F. Bre).

https://doi.org/10.1016/j.enbuild.2021.111251
0378-7788/

1. Introduction

In Brazil, more than 60% of the energy demand is provided by hydroelectric plants [1] and the capacity to supply energy is seriously compromised during the long periods of drought [2]. Therefore, the possibility of supply disruptions due to lack of rainfall is a problem of great importance as was noted in the severe energy crisis of 2001. This forced politicians to establish a series of measures that promoted the development of a regulatory framework for energy efficiency [3].

As in other countries, in Brazil, the building stock has a great potential for energy conservation. In this sense, in 2005 the first standard of national coverage related to the thermal performance of buildings was published by the Brazilian Association of Technical Standards (ABNT). This standard, known as ABNT-NBR 15220 [4], established construction guidelines for single-family public housing to provide building designers with the most appropriate bioclimatic solutions for a given location. With a broader scope, in 2008 ABNT-NBR 15575 [5] was published, aiming at establishing a minimum performance of all residential buildings. This standard approached the building performance within a broader background and also established the first computational method for building performance simulation (BPS) within the Brazilian context. Currently, BPS has also a key role in the energy labeling methods of commercial and residential buildings in Brazil [6]. In addition to requiring the use of BPS in their procedures, these standards were developed and validated based on the use of BPS and metamodels.

Weather data for a location is essential to be able to predict the performance of a given building design through BPS. These data along with occupancy are the most influential boundary conditions in BPS as well as the major sources of uncertainty [7–9]. Ideally, the BPS should be carried out for multiple years (long-term period) of climate data to properly predict the mean performance of the building as well as the peak load demands [10,11]. However, because of the computational effort that this requires, the BPS is usually performed for a single year of hourly data synthesized from long-term statistical weather patterns. This representative year can be an actual calendar year, such as the Test Reference Year (TRY) [12], or a synthetic year defined as the concatenation of 12 Typical Meteorological Months (TMMs) that are statistically representative of the long-term weather conditions. As to this latter, the most accepted definition is the Typical Meteorological Year (TMY) [13,14], and their new versions TMY2 [15] and TMY3 [16].

Given their high relevance for BPS applications as well as the numerical analysis to size sustainable and renewable energy systems, several efforts have been made to develop hourly weather datasets around the world. Apart from the TMY databases [13,15,16] generated by DOE's Sandia and NREL national laboratories, databases of Weather Year for Energy Calculations (WYEC) [17] and International Weather for Energy Calculations (IWEC) [18,19] were generated through ASHRAE projects. Throughout the world, local researchers have generated TMYs in different countries like Nigeria [20], Syria [21], Thailand [22], China [23], Turkey [24], Argentina [25], among others. For further information, Crawley [26], Crawley and Barnaby [27] compare the various weather datasets and review in detail the developments of TRYs and TMYs as well as other climatic data over the past fifty years.

Currently, there is much research focused on the future weather because of predicted climate change and its influence on the performance of buildings or the BPS results [28–30], but unfortunately, only a few studies have addressed the influence of the quality of different data sources of the typical or "current" climate on the BPS results. In one of the pioneer works, Crawley [26] compared BPS results in eight U.S. locations, using 30-year of actual data and different sources of typical weather datasets with hourly data (TRY, TMY, TMY2, WYEC, and WYEC2). He concluded that the TRY-type weather data should be avoided because a single reference year cannot represent the typical long-term weather patterns. The synthetic years (TMY-type) provide results closer to the long-term mean, so they are recommended. Chow et al. [31] performed a similar study for Hong Kong and Macau. Their findings also support the preference of TMY-type over TRY-type data to be used in BPS applications. Additionally, they recommended updating the long-term data use to derive the TMYs including recent weather data, and periodically review this to well reflect the long-term climate change. Erba et al. [32] analyzed the effect of weather datasets on BPS outputs for Milan city in Italy. To this end, they compared five different full-year weather datasets available for Milan and obtained from different sources and periods. Using these data for the BPS a retrofitting analysis of a public building they found very significant differences in terms of energy savings and thermal comfort, particularly noticeable during cooling seasons.

A key climate variable in the TMY definition as well as in the BPS results is solar radiation. However, most weather stations worldwide do not have solar radiation sensors because of their high initial investment and continuing maintenance costs [33]. This lack of measured data led to the development of multiple models to predict solar radiation at different time resolutions depending on their application needs. Therefore, most of the typical meteorological files available for BPS contain calculated solar radiation data. Among others, the IWEC project [18] calculated 11 years of hourly Global Horizontal Solar Radiation (GHSR) data for 227 locations outside the USA using METSTAT (Meteorological/Statistical) clear-sky model [34] and the Kasten Cloudy-sky Radiation Model (CRM) [35]. Zhang et al. [36] proposed an hourly GHSR model (ZHM) and used it to calculate 15 years of data in 28 Chinese locations, which later were expanded to a total of 57 locations [37]. IWEC2 project [19] developed a Koppën-Geiger-based recalibration approach of the ZHM using available measured solar data from a site or sites within each region, to then, be able to predict 25 years of solar radiation data in 3012 locations around the world and derive their TMYs. Bre and Fachinotti [25] used the ZHM calibrated with locally measured data to generate 21 years of hourly GHSR data in 15 locations in northeast Argentina.

Despite its high relevance, there are only a few studies that address and quantify the impact of solar radiation quality because of their modeling on the BPS results. Kim et al. [38] analyzed the BPS results regarding the use of three different GHSR models (CRM, ZHM, and Meteorological Radiation Model (MRM) [39]) for an office building in Busan (South Korea), and the Meteorological Year (MY) of 2010. They found reasonable differences (−0.6% to 4%) in the annual energy consumption for high-performance building design (low solar heat gain coefficient (SHGC) and window-to-wall ratio (WWR)). However, such differences increased to 8% when the SHGC and WWR increased. Recently, Yaman and Arslan [40] investigated the effect of two GHSR models (ZHM and an Angström-Prescott type) on the energy performance of a single-family house assisted with a renewable energy system (photovoltaic panels and solar water heater) in 12 Turkish locations. The original TMYs of each location were modified replacing the measured data with calculated data. Then, these modified files were used in BPS of the single-family house. In comparing the results from the two models, they found a slight deviation in annual heating load intensity (average of 2.5%) but an average deviation of 12.5% for space cooling load intensity.

Even though the previously discussed research presented an interesting approach to the issue under consideration, they have some limitations that are not representative of the real applications. In general, when solar radiation is calculated to generate a TMY, it is done due to a real need for a lack of measured data. So, the solar radiation models, in particular the regression type, are calibrated using a limited set of measured data, to then use such calibrated model to predict the long-term radiation data. Consequently, they are used to predict solar radiation data for non-validated periods, even more, sometimes they are used in near locations to the calibrated or with a similar climate. Furthermore, another feature not analyzed until now, to the authors' knowledge, is how the accuracy of calculated solar radiation influences the generation of the TMY since this variable plays a central role in the selection of the TMMs [13].

For this reason, the main aim of this work is to assess the quality of solar radiation data included in the most recent TMY databases of Brazil and how that quality can influence the selection of TMMs that create the TMY, and consequently, the BPS results. Initially, due to two different modeling approaches were employed, the global horizontal irradiation (GHI) data in the two latest versions of recent Brazilian TMY databases are evaluated, using monthly and daily indicators, against the corresponding satellite-derived ones. In parallel, as another alternative approach, GHSR data are calculated for the same locations and TMYs using the IWEC2 approach (ZHM with the coefficients according to Koppën-Geiger region) and evaluated against the corresponding satellite-derived ones. Then, as both TMY databases are derived from almost the same period, the influence of the solar radiation models in the definition of the TMYs is studied in 92 common locations between the two databases. Finally, to evaluate the impact originating by the different modeling approaches, the BPS results for a set of case studies are exhaustively studied for the whole of Brazil within the local regulations for building performance.

2. Assessment and validation of solar radiation in typical meteorological data

2.1. Climate data for BPS in Brazil

For Brazilian locations, there are currently three main sources of meteorological data processed for use in BPS: Test Reference Year (TRY) database [41], National Institute of Meteorology (INMET) database [42], and TMYx databases [43]. All of them are freely available in the Climate.OneBuilding.Org,[1] repository.

2.1.1. TRY database

This set of meteorological data was developed to be used in BPS for 17 major state capitals in Brazil. The TRY files are single years selected to be most representative. As from a series of raw data provided by ABRAVA (Brazilian Association of Refrigeration, Air Conditioning, Ventilation and Heating) along with CTA/IAE INFRAERO (Aerospace Technical Center - Institute of Aeronautics and Space), with LabEEE [41] revising and formatting the dataset. The raw data was measured in Airports during 1950–1970. The GHSR data was calculated using a regression model based on the total cover information, which was locally developed and calibrated [44]. Apart from the uncertain of the solar radiation source, this database is not usually used because of its low geographic extension, low representativeness of the data, and the age of the data.

2.1.2. INMET database

This set of files, in EPW format, was generated by Maurício Roriz [42] as of the hourly raw data measured at 411 INMET weather stations during 11 years of record (2000–2010). Although the main meteorological variables (including GHSR) used to generate these files were measured by automatic stations, the major part of the raw data was discarded because of the poor quality and large periods of missing data. This drawback limited the proper generation of TMYs for most of the locations, and lead to the creation of single climate years or "TMYs" derived from a short period of record (three to four years), resulting in a set data with very low representativeness of long-term weather patterns.

2.1.3. TMYx databases

TMYx databases, which are developed by Dru Crawley and Linda Lawrie, are freely available in the Climate.OneBuilding repository [43]. TMYx files are typical meteorological years derived from US NOAA's Integrated Surface Database (ISD) [45] with hourly data through 2018 using the TMY/ISO 15927-4:2005 methodologies [14].

Two kinds of TMYs are available in the TMYx databases. First, there are long-term TMYs, derived from the entire available ISD data in each location (up to 82 years in some locations). There are also "recent" TMYs, which are TMYs derived from the most recent 15 years of available and processed data. These latter TMYs aim to represent a recent TMY that includes the latest weather events due to climate change and urbanization. The two kinds of TMYs are differentiated through their names: TMYx for the full dataset and TMYx.year1-year2 for the recent TMYs, which contain a TMYx generation from the period year1-year2.

Of these weather databases for Brazil, the TMYx are the most representative of typical weather patterns for use in BPS [26]. So, these are adopted for the present study. Furthermore, given the fact that TMYs derived from the full dataset can contain years that do not include recent weather events, we decided to focus the study on the recent TMYs files for Brazilian locations.

The latest version of recent TMYs comprises the period 2004–2018. However, this version incorporates a significant change with the previous one regarding the solar radiation modeling for many Brazilian locations by including satellite-derived solar radiation data from the National Solar Radiation Data Base (NSRDB), see Section 2.2. So, both versions are analyzed in this work. Fig. 1 shows the locations compromised in each database.

The methodologies to obtain the solar radiation data for each one of the versions are detailed below.

2.2. Solar radiation modeling approaches

Because the ISD does not have solar radiation data, these must be modeled and calculated. However, there is a significant difference in how solar radiation data were dealt with for a large portion of Brazilian locations, introduced in the latest version of the recent TMYs. This difference is how solar radiation data are modeled as is described below.

2.2.1. TMYx.2003–2017

Within the Brazilian locations, the 175 recent TMY files (see Fig. 1a) of this TMYx version use the modeling approach developed for IWEC data [18]. That is, the GHSR is calculated using the CRM or Kasten's model [35] for the cloudy sky as the function of total sky cover (TSC):

$$\mathrm{GHSR} = \mathrm{GHSR}^0\left(1 - k_1 \mathrm{TSC}^{k_2}\right), \tag{1}$$

where GHSR is given in W/m^2, TSC is given in fractions, GHSR^0 is GHSR under clear sky, which is calculated with METSTAT model [34], and k_1 and k_2 are the regression coefficients that are site-dependent. The default Kasten values were taken from the IWEC report [18].

Finally, the Perez model [46] is fed with the GHSR obtained by the Kasten model to derive the diffuse and direct radiation components.

2.2.2. TMYx.2004–2018

For the 201 recent TMY files of this TMYx version, most locations (136) incorporate GHSR, direct normal, and diffuse horizontal solar radiation data from the NSRDB [47], while the remainder use the same modeling approach just introduced in the previous section. As shown in Fig. 1b, the locations that include NSRDB data are above latitude −20° – the southern-most bounds of the NSRDB. The latest version of the NSRDB includes, among other meteorological data, the GHSR and direct normal component calculated by the Physical Solar Model (PSM) [47]. This model, which was developed through collaboration among NREL, the University of Wisconsin, the National Oceanic and Atmospheric Administration (NOAA), and Solar Consulting Services, is a two-step physical model that

[1] http://climate.onebuilding.org/ a repository of free climate data for building performance simulation.

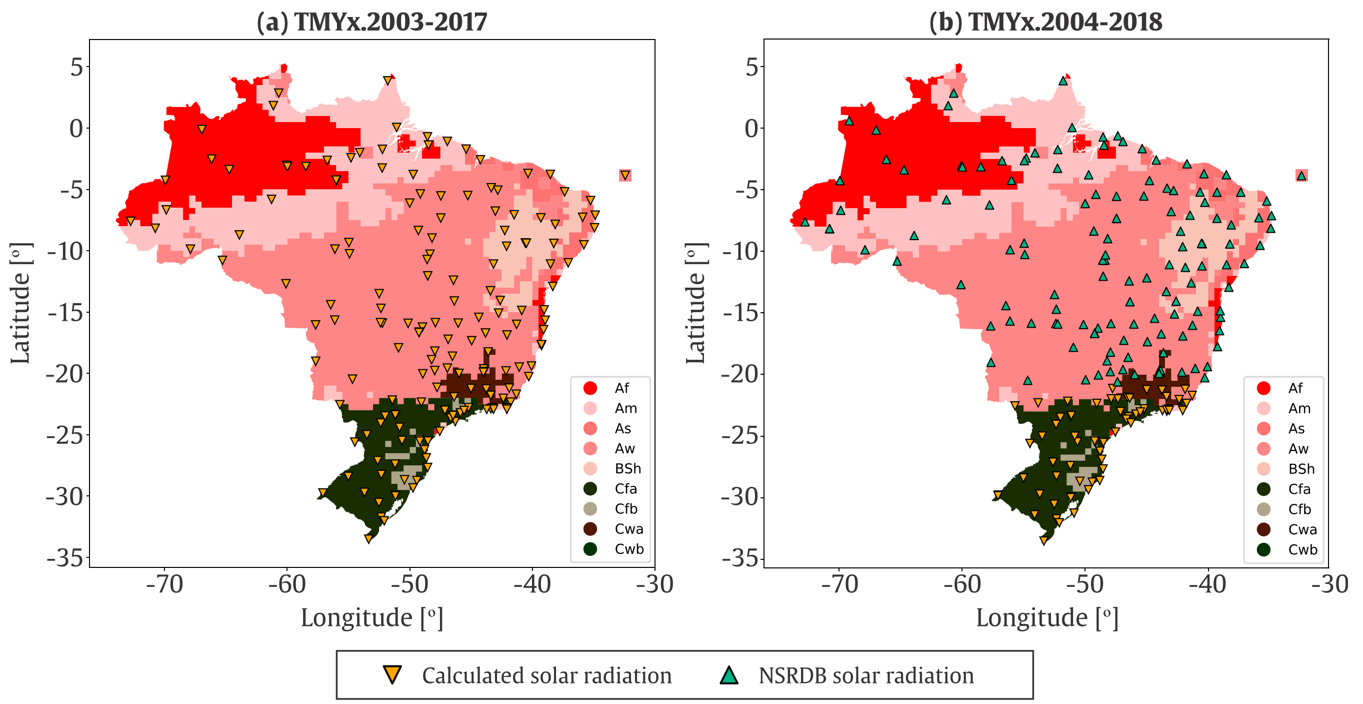

Fig. 1. Locations with recent TMYx files studied in this work. (a) 175 files of the TMYx.2003–2017 database. (b) 201 files of the TMYx.2004–2018 database.

integrates different meteorological data from satellites (aerosol, water vapor, cloud properties, among others) to feed the Fast All-sky Radiation Model for Solar applications (FARMS) [48] to compute GHSR. The solar data comprises a 30-min time resolution for approximately 2 million 0.038-degree latitude by 0.038-degree longitude surface pixels (nominally 4 km^2). For further details regarding PSM see reference [47].

2.2.3. IWEC2 approach

To evaluate the state-of-art GHSR models used to generate TMYs and the influence of the solar radiation source in the BPS results, the IWEC2 modeling approach is also implemented for the same locations and periods within the TMYs. To predict GHSR the IWEC2 project [19] uses the ZHM model [36] with a novel approach for its calibration based on the Koppën-Geiger climate classification.

ZHM defines the GHSR at the hour h as:

$$\mathrm{GHSR} = \max\Big(0, \mathrm{I}_0 \sin \mathrm{SA} \times \Big[c_0 + c_1\mathrm{TSC} + c_2\mathrm{TSC}^2 + c_3(\mathrm{DBT} - \mathrm{DBT}_{h-3}) + c_4\mathrm{RH} + c_5\mathrm{WV}\Big] + D\Big), \tag{2}$$

where GHSR is given in W/m^2, the total sky cover TSC is given in fractions, the dry-bulb temperature DBT is given in degrees Celsius (°C), the relative humidity RH is given in percentage, the wind speed WV is given in m/s, SA is the solar altitude angle, $\mathrm{I}_0 = 1367.7$ W/m^2 is the solar constant, and $D, c_0, c_1, \ldots, c_5$ are closure scalar coefficients; note that all the weather variables in the above equation are measured at hour h, except DBT_{h-3} that is the dry-bulb temperature measured 3 h earlier.

Regarding the values of the closure coefficients, the obtained by the IWEC2 project are employed. These coefficients were calibrated using available measured solar data from a site or sites within each region. A homemade code was implemented to automatically detect the Koppën-Geiger region of each analyzed location, using a spatial resolution of 0.5 degrees (latitude and longitude), as shown in Fig. 1. Within the locations analyzed in both versions of the TMYx databases, nine different Koppën-Geiger regions were detected. The coefficients of ZHM used for these regions are detailed in Table 1. Note that according to IWEC2 the AS and Aw regions have the same set of coefficients because of the lack of measured data to perform the calibration. The detailed results regarding in which region is each location are provided in the supplementary material for closer analysis.

2.3. Validation of the solar radiation models

Validating GHSR data in TMYs for the whole of Brazil is difficult because of the large geographic and temporal extensions required. Furthermore, there is not enough measured data available for the same entire period used in this research. INMET currently has several automatic meteorological stations[2] that measured GHSR. However, it is not easy to access the raw data and most stations were installed after 2008. So, to perform proper validation of the GHSR models, we decided to use GHI satellite-derived data. For source data, we chose the Prediction Of Worldwide Energy Resources (POWER) [49] project by NASA with freely available data.

The POWER Project contains over 200 satellite-derived meteorology and solar energy Analysis Ready Data (ARD), at three temporal levels: daily, interannual, and climatology (derived from the long-term). The POWER database provides data globally at a 0.5 × 0.5° resolution and is updated nightly pursuing to maintain a near real-time availability. POWER data consists of a combination of data resulting from NASA's Applied Sciences Program satellite research programs since 1993, including one of their first activities, the Surface meteorology, and Solar Energy (SSE) project.

The GHI data from the POWER database has been validated against ground-based measurements around the world [50,51]. Regarding Brazilian climates, POWER data has recently been validated against high-quality measurements at a near-equatorial site in Brazil showing low biases error (less than 1%) for long long-term GHI results [52]. Despite this, we decided to include an extra validation of the POWER database in Brazilian climates by its compar-

[2] https://mapas.inmet.gov.br/.

Table 1
ZHM coefficients employed for each Koppën-Geiger climate region according to IWEC2 project [19].

Region	c_0	c_1	c_2	c_3	c_4	c_5	D
Af	0.97136	0.24936	−0.32165	0.03768	−0.00760	0.00794	−2.23175
Am	0.71868	−0.11359	−0.07259	0.01038	−0.00285	0.00866	−8.42023
As	0.80890	0.07355	−0.40101	−0.00424	−0.00242	0.00342	−8.39500
Aw	0.80890	0.07355	−0.40101	−0.00424	−0.00242	0.00342	−8.39500
BSh	0.68149	−0.04697	−0.28420	0.01726	−0.00081	0.00453	−8.91306
Cfa	0.67839	0.03646	−0.39075	0.01359	−0.00148	0.00730	−8.71373
Cfb	0.74370	−0.02988	−0.26353	0.02606	−0.00323	−0.00008	−1.97366
Cwa	0.68175	0.15988	−0.43455	0.01972	−0.00303	0.00201	−6.67731
Cwb	0.65533	−0.00683	−0.13621	0.03240	−0.00252	−0.00320	0.17022

ison against high-quality ground measurements from the Baseline Surface Radiation Network (BSRN) database [53], see Section 2.4.1.

Therefore, by this approach, daily GHI is processed for the same locations (latitude and longitude) as well as the days of the corresponding TMMs that constituted the analyzed TMYs. It is worth noting that the NSRDB data, which were included in some locations of the latest version of the TMYx (2004–2018), use the same source of satellite-derived data as POWER does. However, by adopting the POWER data as the standard a proper validation can be performed for the two recent TMYx databases and in all the analyzed Brazilian locations.

The validation of the different GHI sources is performed as described in Fig. 2. To this end, the daily GHI, and the monthly mean daily GHI indexes are employed. So, for the hourly GHSR data (IWEC, NSRDB, or IWEC2), the daily GHI values are obtained as the sum of the GHSR for the 24 h of the day. Finally, the monthly mean daily GHI index is obtained by averaging the daily GHI values of the corresponding month.

2.3.1. Performance assessment

All the validation of models through any index of GHI data is carried out using the normalized root mean square error (nRMSE) and the normalized mean bias error (nMBE) as described below,

$$\mathrm{nRMSE} = \frac{\sqrt{\overline{(x_{mod} - x_{std})^2}}}{\overline{x_{std}}}, \quad (3)$$

$$\mathrm{nMBE} = \frac{\overline{x_{mod} - x_{std}}}{\overline{x_{std}}}, \quad (4)$$

where x_{mod} represents the values of GHI obtained by different models/sources (IWEC, NSRDB, IWEC2, or POWER) and x_{std} are the corresponding ones taken as standard (POWER or BSRN) in each case.

2.4. Results

In this Section, a quantitative measure of the quality and accuracy of the solar radiation models employed in Brazilian TMYs is performed. Initially, a validation of the POWER database for Brazilian climates is carried out by comparison of the GHI values against BSRN data in four locations. Then, the GHI of the TMYs derived from the period 2003–2017 are analyzed against the POWER database. Finally, the same analysis is carried out for the TMYs derived from the period 2004–2018. Parallelly, the GHI obtained using the solar radiation approach developed by the IWEC2 project is also assessed for the same TMY locations and periods.

2.4.1. Validation of POWER data

As said before, a previous validation of the POWER database is performed through the comparison of GHI data against the ones derived from four Baseline solar radiation stations in Brazil. These cover strategic regions of Brazil and are located at the cities of Brasilia [54], Florianópolis [55], Petrolina [56], and São Martinho da Serra [57].

Starting from the raw BSRN data for each location, a first filter is applied to just keep measurements within the period of interest of this work (2003–2018). After this, the minute resolution raw data is processed to hourly GHSR as the mean value within the hour. Then, the daily GHI values are calculated as the sum of the hourly values during the day but keeping only the complete days, i.e., days with 24 measurements of hourly solar radiation. Finally, the monthly mean daily GHI is calculated by averaging the daily GHI values of the corresponding month but calculating only those months that have at least 28 days of measured data.

Table 2 shows a summary of the BSRN data before and after processing by using the methodology previously described.

Fig. 3 shows the agreement between POWER and BSRN databases for the monthly mean daily GHI at the four locations in Brazil. From these results, it can be seen that POWER data presents a very good prediction of GHI at the four locations, showing R^2 of 0.91 to 0.99 as well as nMBE and nRMSE lower than 5% except to Petrolina location where nRMSE is 5.79% mainly driven for a bias error. However, given the particularity of this bias error only for Petrolina location, it is highly probable that the source of it comes from the calibration of the station instruments.

Therefore, given the general good accuracy of GHI from the POWER database, this source is taken as the standard to perform the rest of the validations in this work.

2.4.2. Period 2003–2017

To introduce a general insight into the solar radiation model accuracy, Fig. 4a shows the monthly mean daily GHI indexes of the solar data in the TMYx.2003–2017 files, which was obtained by the IWEC modeling approach, against the corresponding ones derived from the POWER database (satellite) in the 175 locations. Fig. 4b shows the equivalent comparison for the data obtained via the IWEC2 approach in the same TMYs.

The data obtained by the IWEC approach presents an nRMSE of 17.18% and an nMSE of 11.39% regarding the POWER data. This indicates an acceptable prediction but with an overestimation, particularly for the highest values of GHI. The data obtained through the IWEC2 approach has a lower nRMSE (13.12%) and nMSE (-3.71%), which indicates a general better prediction with a slight underestimation.

To perform a deeper analysis, Fig. 5 shows a bar plot of the nRMSE and nMSE errors of each modeling approach (see Fig. 5a and Fig. 5b, respectively), but with the errors computed for each month of the year and in all the locations. The IWEC2 approach has good performance for all months with a slightly better prediction during winter months, achieving nRMSE $<$ 15% for all the months except for October. Furthermore, the nMSE is observed to be bounded with a low value ($\simeq$5%), showing a general underestimation for all the months except for October where the radiation is very slightly overestimated.

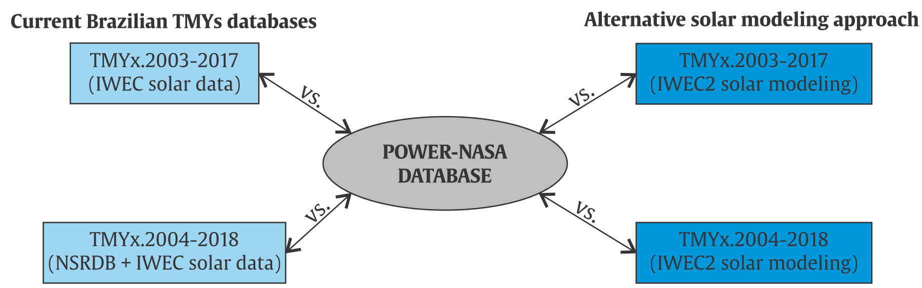

Fig. 2. GHI validation scheme.

Table 2
Summary statistics of the BSRN data before and after processing.

Location	Total of months	
	Raw data	Processed data
Brasilia	155	45
Florianópolis	191	52
Petrolina	143	71
São Martinho da Serra	155	102

On the other hand, the radiation in the TMYx has a very good performance (nRMSE < 10%) for winter months but the errors increase as the summer months approaches, giving an nRMSE above 20%. TMYx values present a general overestimation of the radiation, which is also more noticeable during the summer months.

To focus on the accuracy of radiation modeling approaches at the location level, Fig. 6a and d show histograms of the nRMSE dis-

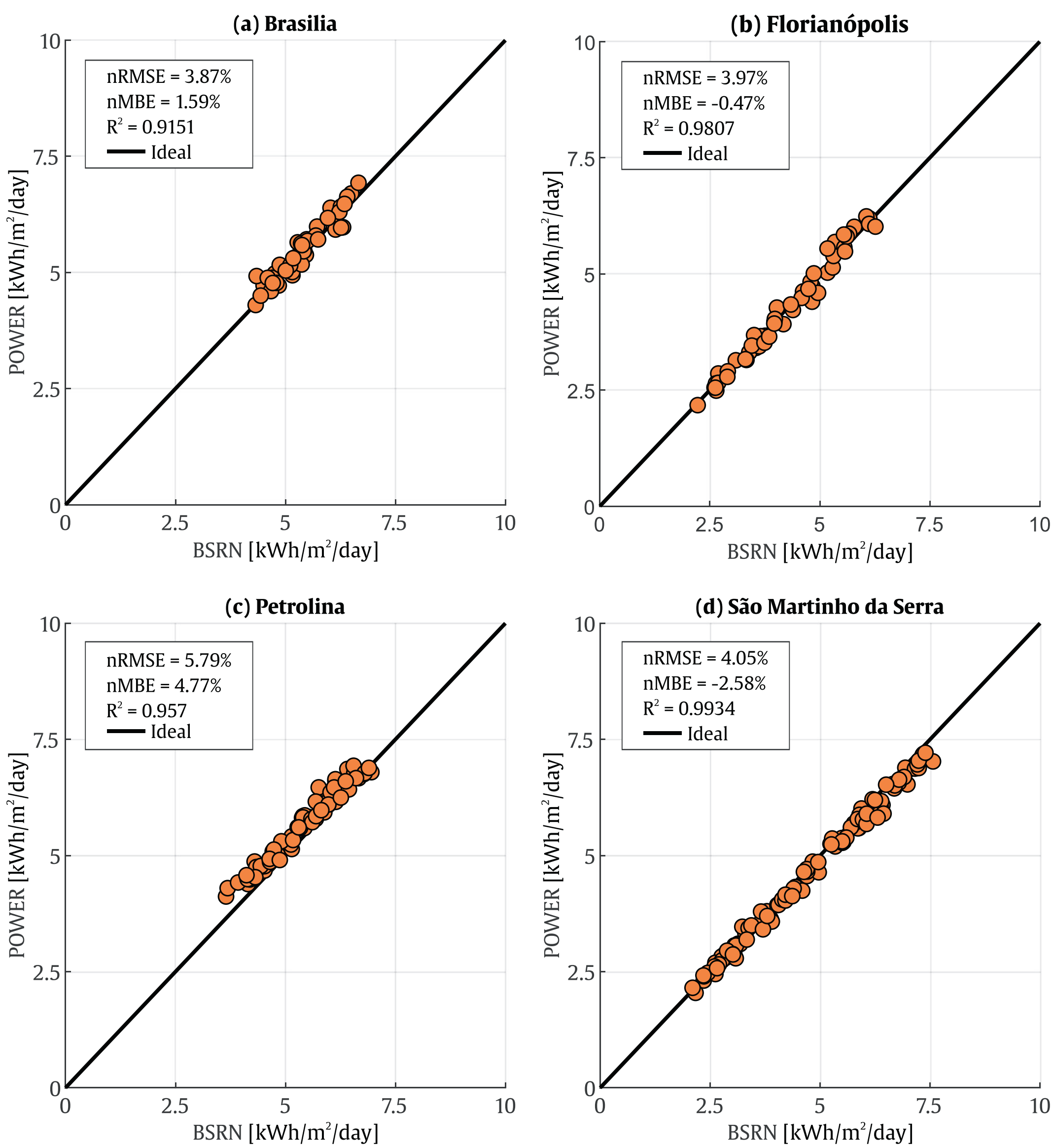

Fig. 3. Agreement between POWER and BSRN databases for monthly mean daily GHI at four locations in Brazil.

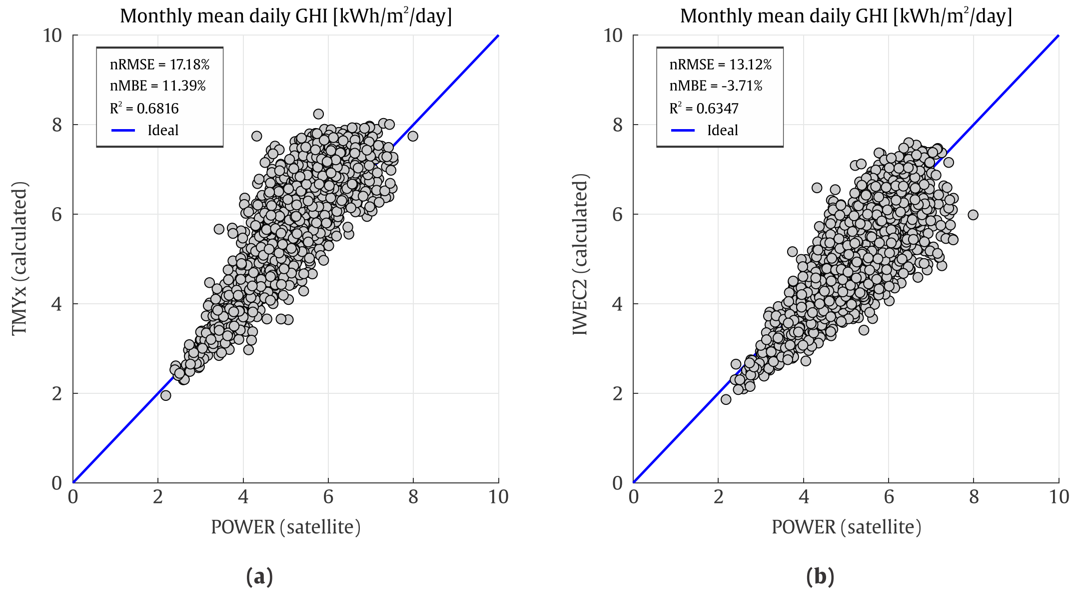

Fig. 4. Comparison, using monthly mean daily GHI index, of calculated solar radiation against the satellite derived (POWER) ones for the TMYs derived from the period 2003–2017. (a) TMYx models (IWEC approach). (b) IWEC2 approach.

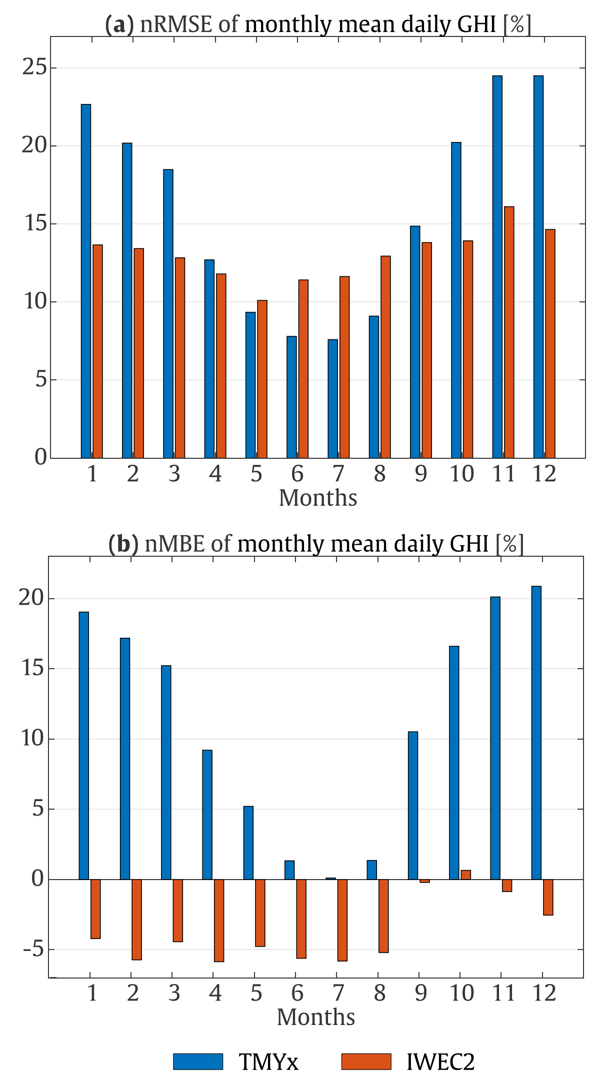

Fig. 5. Error bar plot of the radiation modeling approaches through the monthly mean daily GHI index for the TMYs derived from the period 2003–2017. (a) nRMSE; (b) nMSE.

tribution for the monthly mean daily GHI at each location using the TMYx (IWEC) and IWEC2 approach, respectively.

When using the IWEC approach, many locations (above 30%) have an nRMSE between 15 and 20%. But, about 25% of the locations have an nRMSE between 10 and 15% and approximately 15% between 5 and 10%. This indicates that more than 70% of locations have an nRMSE ⩽20%, and the rest have a 20%<nRSME<35% with only a few locations above 30%.

For the IWEC2 approach, many locations (above 40%) have an nRMSE between 5 and 10%, more and less 35% of the locations between 10 and 15%, and about 15% between 15 and 20%. This means that more than 90% of locations have an nRMSE ⩽20%, while the rest of the locations (<10%) have an nRMSE between 20 and 30% and no location is above 30% nRMSE.

This analysis allows a quick insight into the accuracy of the radiation modeling approaches. However, although the monthly mean daily GHI is a commonly employed index, the performance of buildings is more related to the dynamical physical phenomena at lower scales of time like hourly values. In this sense, Fig. 6b and e show the equivalent histograms but with nRMSE computed using the daily values of GHI (highest resolution time scale provided by the POWER database).

From these results, the nRMSE distribution considerably varies and their values increase in general for both approaches, which indicate that monthly indices can be very general, especially for BPS analyzes. For the TMYx approach, most locations (above 90%) have an nRMSE between 15 and 35% while a few locations (≃5%) have an nRMSE of 35–45%. On the other hand, the IWEC2 approach has better performance since most of the locations (≃90%) have an nRMSE between 15 and 30% while few locations (≃10%) have nRMSE of 30–40%.

To give a geographical idea of the accuracy of both approaches and achieve a deeper understanding of this, Fig. 6c and f show contour maps of nRMSE for daily GHI throughout Brazil. For TMYx, see Fig. 6c, it is observed that the prediction of daily GHI in most of Brazil has an nRMSE between 25 and 30%, particularly for the central northern regions. This means that solar radiation modeling employed in TMYx has low accuracy in “tropical” locations, a shortcoming already noticed in the IWEC project [18]. This aspect is improved by the IWEC2 approach since the nRMSE for these regions is 20–25%, see Fig. 6f.

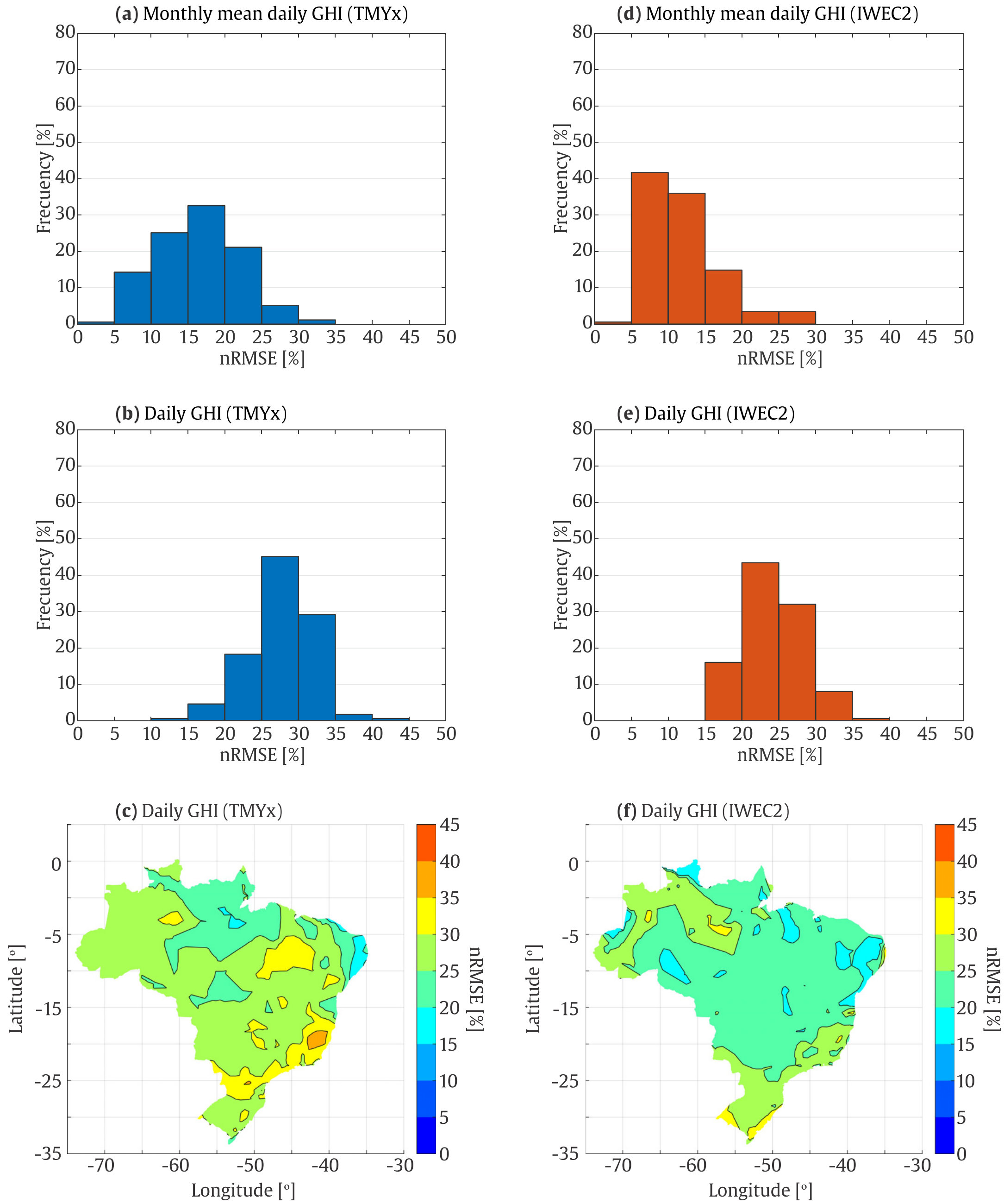

Fig. 6. Distributions of nRMSE for the TMYs derived from the period 2003–2017.

2.4.3. Period 2004–2018

In this Section, the equivalent results to those previously discussed for both approaches (TMYx and IWEC2) are analyzed but for the TMYs derived from the period 2004–2018. It worth remembering that TMYx.2004–2018 incorporates an important change regarding the incorporation of solar radiation data from the NSRDB database in northern locations as exposed in Section 2.2 and is shown in Fig. 1b.

Fig. 7 shows the fit of the monthly mean daily GHI of the POWER database and both modeling approaches (TMYx and IWEC2). As was expected, the TMYx radiation data considerably improve their accuracy by incorporation of the NSRDB decreasing the nRMSE to 8.6% and the nMSE to 4.59%.

Regarding the performance of the IWEC2 approach for these TMYs, it slightly decreases the nRMSE to 12.15% and almost keeps the nMSE with a value of -4%. This indicates good robustness of the radiation modeling approach for a wide range of different years and inputs, see Section 3.2.1 for further details.

Fig. 8 shows a bar plot of the nRMSE and nMSE errors for the monthly mean daily GHI index, splitting these by month and for each modeling approach.

As to the accuracy of both approaches in terms of the monthly mean daily GHI, TMYx data present very good performance with an nRMSE $< 10\%$ for most of the months except for October, November, and December when nRMSE sightly overcomes the value of 10%. On the other hand, the IWEC2 approach presents a good performance with nRMSE $< 15\%$ for all the months including nRMSE $< 10\%$ for winter months.

Regarding the prediction deviation interpreted through nMSE, both approaches present very good performances (nMSE $\leqslant |8\%|$), showing almost an opposite behavior, that is, a general overestimation by the TMYx and underestimation by the IWEC2.

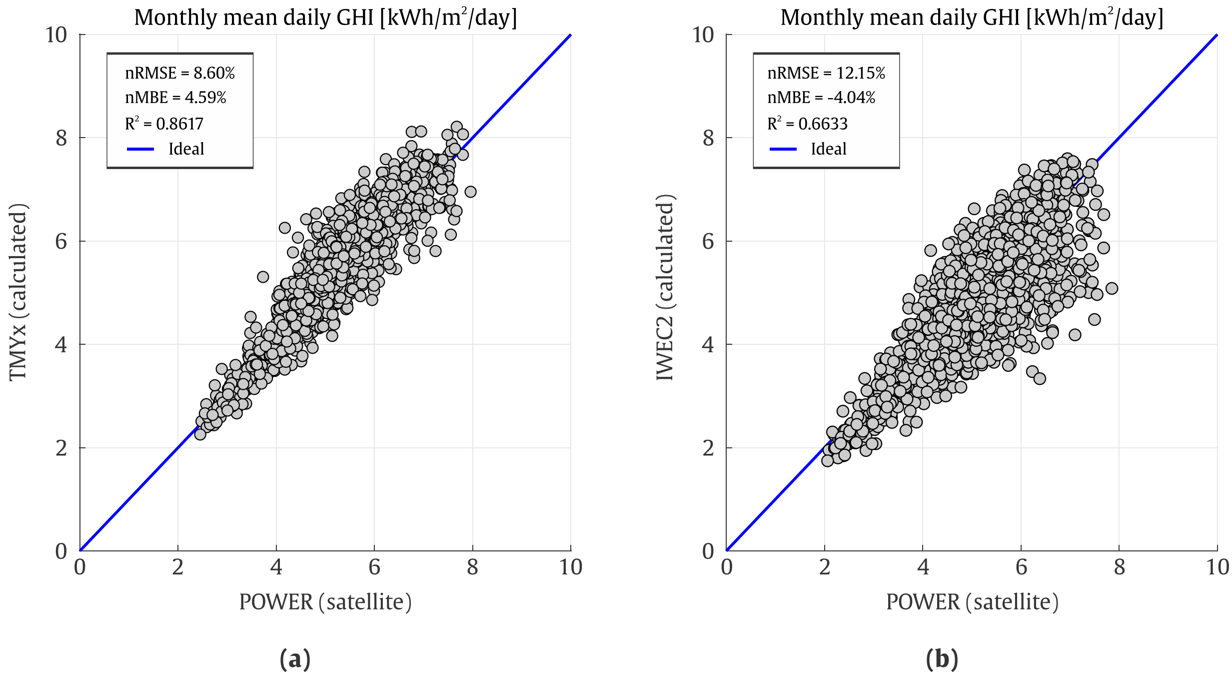

Fig. 7. Comparison, using monthly mean daily GHI index, of calculated solar radiation against the satellite derived (POWER) ones for the TMYs derived from the period 2004–2018. (a) TMYx models (IWEC approach). (b) IWEC2 approach.

Fig. 9a and d show histograms of the nRMSE distribution for the monthly mean daily GHI at each location using the TMYx and IWEC2 approach, respectively. Both approaches improved their performance relative to the results obtained for the TMYs derived from the period 2003–2017.

Regarding the accuracy in terms of daily GHI of the TMYx data, these have ≃80% of locations with an nRMSE between 10 and 25%, ≃18% of locations with an nRMSE of 25–30%, and the rest (<5% of locations) presents an nRMSE between 30 and 35%, see Fig. 9b. Geographically, it can be observed that most of Brazil shows an nRMSE between 15 and 20% for this approach, see Fig. 9c. Particularly, this good performance is observed in the central northern regions, which means a significant improvement relative to the previous modeling approach (IWEC) using in the period 2003–2017. From Fig. 9c it can also be seen that the regions with major values of nRMSE (25–35%) are small in size and are located in the South of the country where the NSRDB is not available and the radiation is still modeling by the previous approach (IWEC). Another known issue in the satellite-derived data is that they are not as accurate in coastal areas.

As to the daily GHI results of the IWEC2 approach for the same periods and locations, ≃75% of locations have an nRMSE between 10 and 25%, ≃18% of locations with an nRMSE of 25–30%, ≃5% with an nRMSE of 30–35% and the rest (<5% of locations) presents an nRMSE between 35 and 45%, see Fig. 9e. Geographically, it can be observed that most of Brazil present acceptable performance with an nRMSE between 15 and 25% for this approach, see Fig. 9c. From this figure, it can also be seen that the regions with major values of nRMSE (above 30%) are small in size and are mainly placed nearby to the bounds of the Koppën-Geiger region employed, e.g., along the western border where the country limit with a sea coast. Based on this appreciation, it could be possible to improve this issue by using a better grid resolution for the region detection.

2.4.4. Discussion

This section aims to briefly discuss the potential physical reasons for the differences in the performance of the two main solar modeling approaches herein evaluated, IWEC and IWEC2. In the IWEC approach, Kasten's model is employed to predict GHSR for cloudy sky hours, see Eq. (1). This model modifies the GHSR under clear sky hours as a function of total sky cover information. Regardless of the accuracy of the GHSR under clear sky hours, if cloud cover information has complex behavior or this data has poor quality, the model cannot overcome this issue during cloudy hours. On the other hand, the IWEC2 employs the Zhang-Huang model under any sky conditions, see Eq. (2). This model, apart from considering the cloud cover information also includes other climate variables like dry-bulb temperature, humidity, and wind speed. These extra terms allow obtaining more stable performance on the prediction of GHSR even under complex cloud cover situations. This means the extra terms can implicitly capture more complex cloudy sky hours conditions or compensate in the case that cloudy information has poor quality. This feature results in a more robust performance for different real scenarios.

In the cases evaluated in this work, the aforementioned aspects can be particularly noticeable for two reasons: i) most of the climate regions are hot and humid with a complex cloud cover behavior, and ii) most of the cloud cover information is obtained through a human-observation-based approach in Brazil.

These aforementioned physical-mathematical features of the models are the reasons that drive that the IWEC approach has larger differences in summer months (higher values of GSHR) and a general overestimation as well as the IWEC2 approach has a more stable performance throughout the year, see Figs. 4 and 5. More advantages and disadvantages of these widely employed solar modeling approaches should be analyzed in a dedicated work including more diverse climate conditions.

3. Influence of solar radiation modeling on the TMY generation and the BPS results for Brazil

This Section aims to assess and quantifies the impact of solar radiation modeling on TMY generation and the BPS results for the whole of Brazil. The methodology is summarized in Fig. 10.

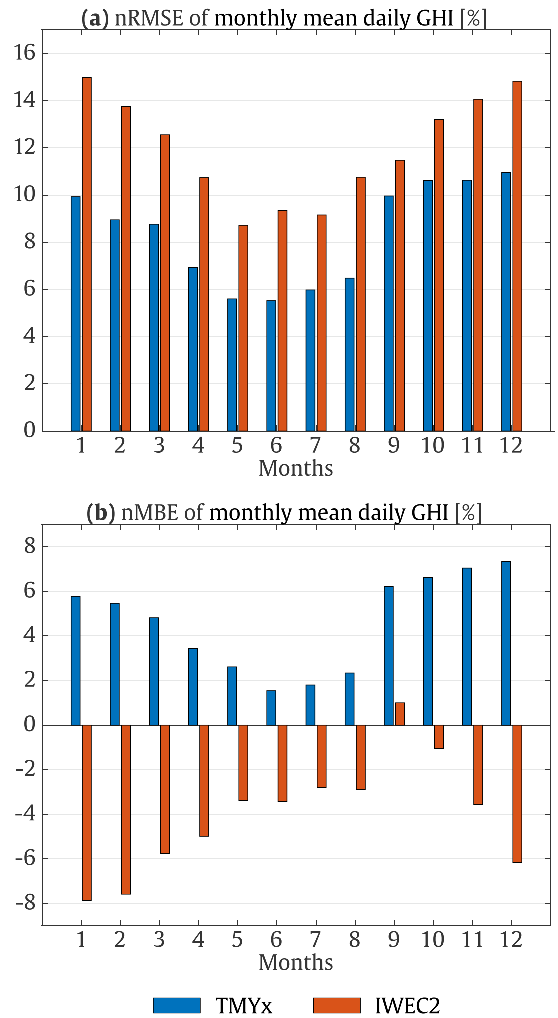

Fig. 8. Error bar plot of the radiation modeling approaches through the monthly mean daily GHI index for the TMYs derived from the period 2004–2018. (a) nRMSE; (b) nMSE.

First, to evaluate the influence of the radiation modeling on the generation of actual TMYs within Brazilian climates, an analysis of the TMY configurations is carried out in 92 locations. These are common locations between the TMY databases analyzed (TMYx.2003–2017 and TMYx.2004–2018) that have changed the solar modeling approach between them, i.e., from IWEC to NRSDB approach.

Then, four typical case studies within the current Brazilian regulations for building performance, two residential and two commercial buildings, are simulated to analyze and quantify how the changes of TMY configuration because the radiation modeling influences the BPS results.

Finally, to isolate the effect of solar radiation modeling on the BPS results, the TMYs for both periods are modified with the radiation obtained through the IWEC2 approach in the 92 locations, and the four case studies are also simulated with these files.

3.1. BPS case study buildings

The case study buildings chosen are representative of typical designs analyzed within the Brazilian regulations for energy and thermal performance of the residential and commercial buildings. In both current standards, the performance of the target building to be analyzed (real model) has to be compared against the performance of its reference model, whose main construction components are previously established by the corresponding normative.

Therefore, the influence of solar radiation data on the final BPS results of the target building and its reference models are studied here for both, residential and commercial buildings. The models to represent these case study buildings were generated and simulated in EnergyPlus software version 9.2.0 as described in the next sections.

3.1.1. Residential buildings

The residential building sector is represented by a single-family housing of social interest (see Fig. 11) that depicts one of the archetypes employed in the development of the last update of NBR 15575 [58]. The main settings of the EnergyPlus model for the real building and its reference model are detailed in A.4 of the Annex A, showing construction components, geometric characteristics, and other model settings.

A common operation mode employed in Brazilian residential buildings is the hybrid-conditioning mode. This operation mode aims to exploit natural ventilation strategy during hours that it is possible and use air-conditioning when natural ventilation is not enough. In this sense, an innovative methodology to simplified evaluates such hybrid operation mode in residential buildings was introduced in the last update of NBR 15575 [58]. This methodology is based on two separate and sequential simulations, one with only natural ventilation and another using only artificially air-conditioned. By using this approach, it is possible to evaluate such hybrid operation mode through two simple simulations able to be performed by an engineer, architect, or technicians without the need to use advanced controls like the Energy Management System (EMS) of EnergyPlus.

The first simulation, the naturally ventilated model, aims to establish the periods of occupied hours where the operative temperature (T_{op}) is outside a pre-established range limit, which is considered here as 18 °C$\leqslant T_{op} \leqslant$26 °C for all Brazilian climates. So, this simulation establishes the hours when natural ventilation is not sufficient to promote thermal comfort, indicating the need for artificial conditioning. Then, these periods of "uncomfortable" occupied hours are used to calculate the annual ideal loads according to the second simulation, the artificially conditioned model, which has a setpoint temperature of 21 °C for heating and 23 °C for cooling.

From the first simulation, apart from determining the periods that artificial conditioning is necessary, the percentage of hours within the preset range of operative temperatures (PHWOT) is also obtained, being is established as the average of the percentage calculated for each of the thermal zones that can be conditioned, i.e. living room and bedrooms. A high value of PHWOT indicates that the T_{op} is within the preset range for most of the occupied hours (good performance) and vice versa. From the second simulation, the ideal thermal loads of each room environment are summed for the hours determined in the first simulation to establish the performance indicator of the artificially conditioned house. Both of these indicators are also analyzed in this work. Fig. 12 shows a schematic example of the simplified methodology based on the two separate and sequential simulations to evaluate the hybrid operation mode.

The natural ventilation modeling is carried out through the AirFlow Network (AFN) model of EnergyPlus. Due to the case study is a gable-roofed building and its shape is not exactly rectangular, and also, the target building model has eaves, the wind pressure coefficients (C_p) for both buildings (target and reference) are calculated using CpSimulator platform [59]. Besides being able to predict the C_p data for general shape buildings using advanced computational fluid dynamics tools, this platform automatically

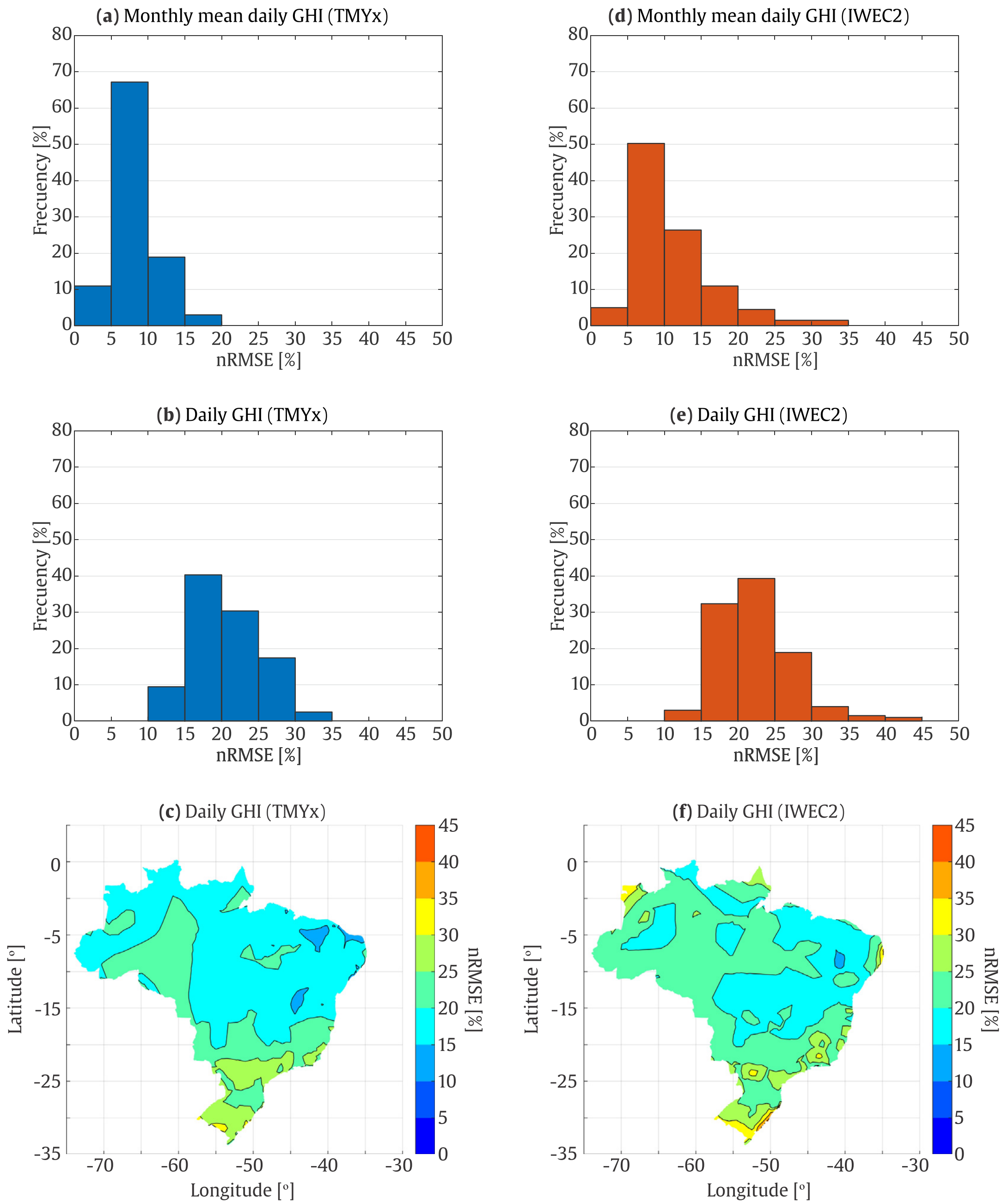

Fig. 9. Distributions of nRMSE for the TMYs derived from the period 2004–2018.

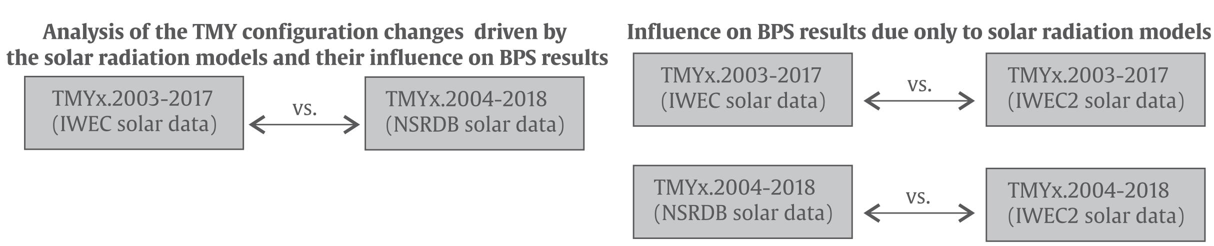

Fig. 10. Influence of solar radiation modeling on the TMY generation and the BPS results for Brazil.

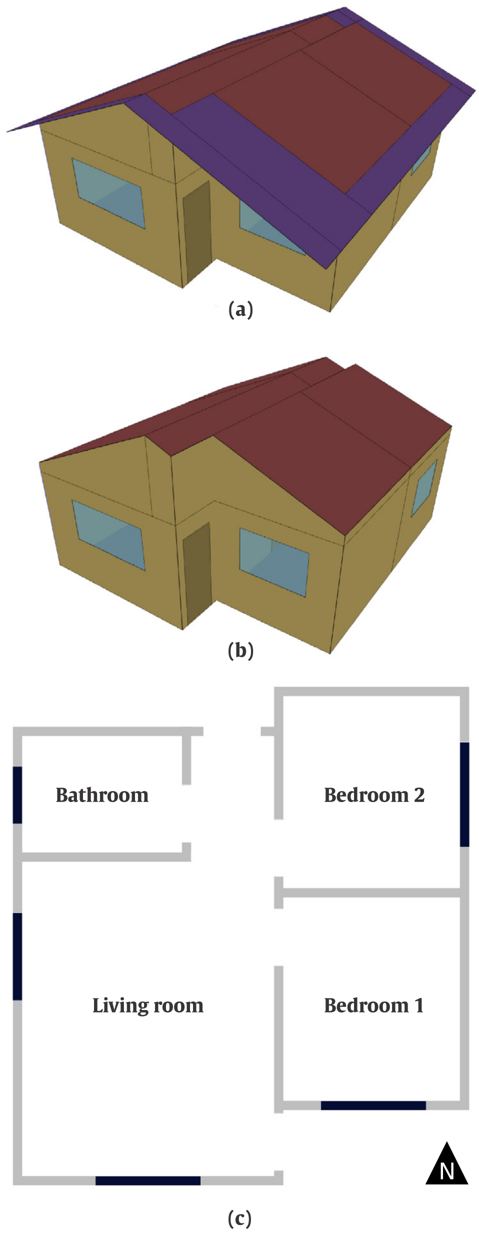

Fig. 11. Residential building models used in comfort and thermal load simulations: (a) target building; (b) reference model; (c) floor-plan view.

computes the average C_p on the opening areas. So, an external node and the set of C_p for 12 wind incidence angles (every 30°) are used for each external opening. The windows opening control is based on temperature, that is, they are open whenever the outside temperature is higher than 19 °C and the inside temperature is higher than the outdoor air temperature. Some openings always remain closed, as is the case with the external doors and the bathroom door. On the other hand, some openings always remain open, as is the case with the internal doors of the other rooms and the bathroom window. In this way, the calculation of the percentage of hours in comfort is performed through the hours when the internal operative temperature of each environment was between 18 and 26 °C, considering only the occupied hours. The main settings of both simulations, naturally ventilated and artificially conditioned, are detailed in Table 3.

Regarding occupancy schedule, the same pattern is observed every day of the year, where from 2 pm to 6 pm the room has 50% of the occupancy rate, from 6 pm to 10 pm this rate is 100%, and from 10 pm to 8 am the bedrooms have 100% of the rate. For example, 100% of the living room occupancy rate equals 4 people and 100% of the bedroom equals 2 people. In addition, this same pattern is used to represent the use of the living room and bedroom lighting system, where 100% represents 5 W/m^2. However, electrical equipment is only present in the room and its percentage is always equal to 100 in the occupation period, which represents 120 W.

3.1.2. Commercial buildings

The commercial sector is represented by an office building with four perimeter zones and a core zone (see Fig. 13). This model was used in studies that comprised the development of the current Inmetro Normative Instruction for the classification of energy efficiency of commercial, services, and public buildings (INI-C) [60]. This regulation also establishes that the office performance (target building) must be compared with an office building with reference characteristics prescribed in the standards. As in the residential case study, the reference represents a building with lower energy efficiency, which allows verifying the impact of the uncertainty associated with solar radiation in commercial buildings with different levels of performance.

The main settings for BPS of this office building using EnergyPlus are described in A.5 of the Annex A. Following the INI-C normative, the building is assumed to only use artificial conditioning, with a setpoint temperature of 18 °C for heating and 24 °C for cooling. The Heating, Ventilation, and Air-Conditioning (HVAC) system only works during periods when the building is occupied and the building performance indicator is

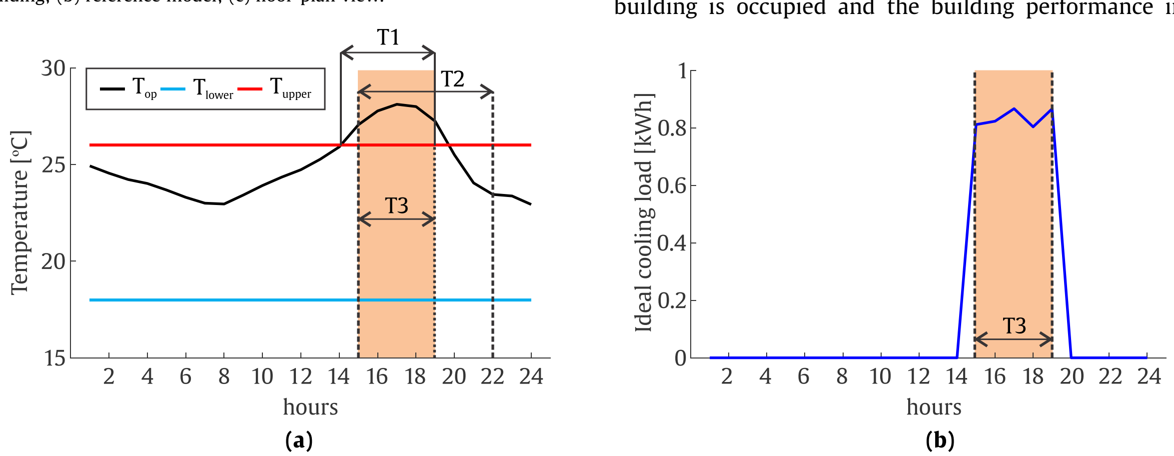

Fig. 12. Example of simplified methodology to evaluate the hybrid operation mode in residential buildings. T1 = period out of range, T2 = occupied period, T3 = occupied period out of range. The results are for the living room of the case study during March 28 in Porto Alegre (WMO = 839710). (a) Temperatures of the naturally ventilated model; (b) Period to sum the thermal ideal loads for cooling.

Table 3
Summary of main settings for the naturally ventilated and air-conditioned simulations.

Simulation	Details	Target building	Reference building
Naturally ventilated (sim 1)	Type modeling	AFN	
	Wind Pressure Coefficient Type	Input	
	Opening factor	0.90	0.45
	Discharge Coefficient	0.6	
	Window: Air Mass Flow Coefficient When Opening is Closed [kg/(s m)]	0.00063	
	Window: Air Mass Flow Exponent When Opening is Closed	0.63	
	Door: Air Mass Flow Coefficient When Opening is Closed [kg/(s m)]	0.00024	
	Door: Air Mass Flow Exponent When Opening is Closed	0.59	
Air-conditioned (sim 2)	Type modeling	Ideal loads	
	Heating setpoint [°C]	21	
	Cooling setpoint [°C]	23	
	Dehumidification	No	
	Outdoor Air Flow Rate per Person [m^3/s]	0.00944	

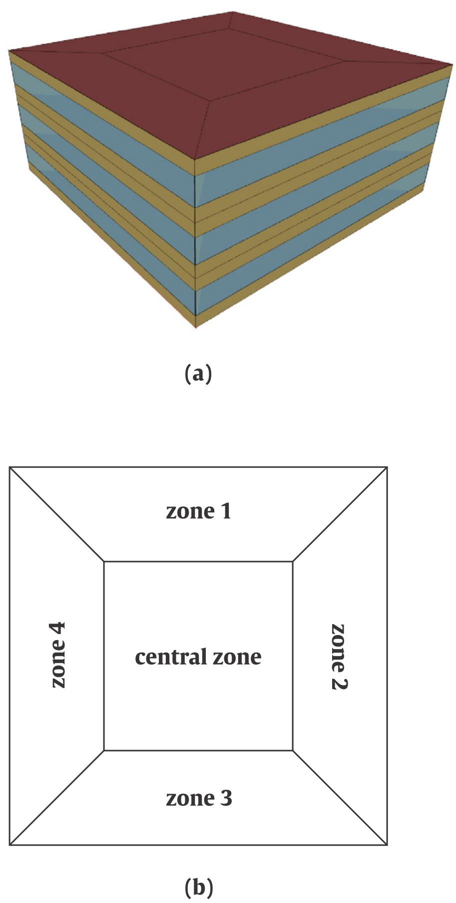

Fig. 13. Commercial building models used to ideal thermal load simulations.

obtained by summing the ideal thermal load of all thermal zones. The normative defines office buildings are open from Monday to Friday, from 8 am to 12 pm with 100% occupation, from 12 am to 1 pm with 50% occupation, and from 1 pm to 6 pm with 100% occupation, according to the values shown in Table A.5. The period of occupation also defines the pattern of use of electrical equipment and the lighting system.

3.2. BPS results

3.2.1. TMY generation

As we mentioned earlier, we assessed the TMY configurations for 92 locations common between the TMY databases analyzed (TMYx.2003–2017 and TMYx.2004–2018) that have changed the solar modeling approach from IWEC to NRSDB. Note that these sets of TMYs were developed using the same TMY generation methodology based on ISO 15927–4:2005 [14] and derived from a very similar period (2003–2017 and 2004–2018) having 14 of 16 years in common. Consequently, we expect that TMY configurations do not change significantly. It worth mentioning that the ISO method does not employ different weighted factors as the well-known TMY and IWEC methodologies, giving the same importance to the three primary variables, see [61] for further details.

Fig. 14 shows a histogram of the percentage of locations that keep the same typical meteorological month (TMM) between both versions. The TMMs that have suffered the fewest changes is February. However, 87% of locations change the year selected for this TMM. This indicates that solar radiation modeling is highly influential in the selection of the TMMs and the final TMY configurations.

To have extra physical information about the resulting TMYs in the TMYx.2003–2017 and TMYx.2004–2018 databases at the 92 locations, Fig. 15 shows a correlation analysis for the primary weather variables between both databases. Despite the several changes of the TMY configurations the dry bulb temperature and relative humidity keep a good correlation between both databases (R^2>0.85), while the GHI presents a lower correlation (R^2=0.59). These results indicate that the major changes of the TMY configurations driven by the solar radiation data mean mainly major changes in GHI values of the resulting TMYs but those do not significantly affect other primary variables like temperature and humidity.

3.2.2. Influence on BPS results due to changes of TMY configurations driven by the solar radiation models

As was introduced before, the accuracy of solar radiation modeling can highly influence the resulting TMY configurations. So, this section aims to evaluate the impact of such TMY configuration changes on the BPS results, particularly, for the residential and commercial case studies within Brazilian regulations that were described in the previous sections.

Residential buildings Fig. 16 shows the comparison of the BPS results for the target residential building using TMYx.2003–2017 and TMYx2004–2018 databases in the 92 analyzed locations. Particularly, the agreement of the results for the annual PHWOT index is shown in Fig. 16a and for the annual ideal loads in Fig. 16c. Considerable errors are observed in some locations for both indicators resulting in nRMSEs of 29.62% and 20.9% for annual PHWOT and ideal loads over all the locations, respectively. It is worth noting that annual ideal loads for residential and commercial buildings in Brazil consist almost of only cooling loads, especially for the 92 locations herein analyzed. So, the following analyses are just

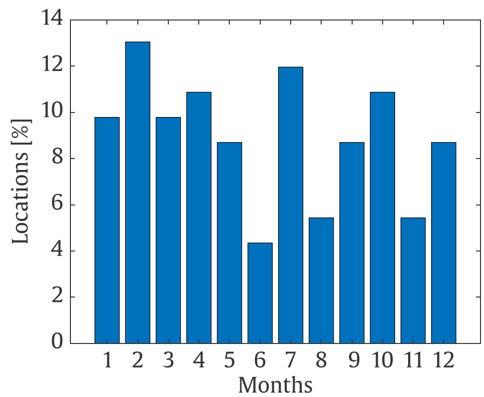

Fig. 14. Percentage of same TMMs between the TMYx.2003–2017 and TMYx.2004–2018 databases.

focused on total loads instead of split them into heating and cooling loads.

The distribution of the normalized differences (nDiff) between the results obtained with both databases can be observed in Fig. 16b and d for the annual PHWOT and annual ideal loads in the target building, respectively. It can be seen that most of the locations ($\simeq$ 65%) present a $|\text{nDiff}| < 20\%$ for both indicators, however, the results for few locations show large differences between TMY databases, this means a nDiff $>$ 40% for annual ideal loads and nDiff $>$ 60% for the annual PHWOT.

Fig. 17 shows the same analysis as Fig. 16 but for the reference model of the residential case study. Regarding the annual PHWOT, the differences between BPS results obtained with both TMY databases are largest than for the target building, resulting in an nRMSE = 50.46% over all locations, see Fig. 16a. The distribution of nDiff for PHWOT shows that there are various locations with large differences and that for a few of these the nDiff can be upper 130%, see Fig. 16b. This indicates that the PHWOT employed in residential buildings is highly sensitive to the climatic boundary conditions and that this is more noticeable when the analyzed building has a low performance like the reference one.

As to the agreement of annual ideal loads between both TMY databases for the reference model, differences are lower than for the target model, indicating an nRMSE = 14.65% over all the locations, see Fig. 16c. The distribution of differences shows that $|\text{nDiff}| < 40\%$ for all locations, concentrating most of the locations ($\simeq$ 80%) with a $|\text{nDiff}| < 20\%$.

Other important indicators to characterize the performance of buildings are the peak loads. Fig. 18 shows the distribution of nDiff for the peak cooling loads in the residential case studies using both databases (TMYx.2003–2017 and TMYx.2004–2018). Contrastingly with PHWOT and annual loads, it can be seen that cooling peak loads are not highly affected by the use of both TMY databases, this is, in most locations (80%) the $|\text{nDiff}| < 20\%$. This low influence of the use of the different TMYx databases on the peak cooling loads for residential buildings is associated with the low internal gains of these building typologies, i.e., the max undesired values like the peak loads are not too much sensitive to the climate conditions.

Commercial buildings Fig. 19a–d shows the agreement of annual ideal loads calculated for the target office building and its reference model using TMYx.2003–2017 and TMYx2004–2018 databases in the 92 analyzed locations. The differences obtained for both office buildings (target and its reference) due to the changes of TMY configuration between both databases are much lower than for the residential ones, accusing nRMSE $<$ 7% over all locations in both cases, see Fig. 19a and 19c. The distribution of normalized differences is also similar between both case studies with a $|\text{nDiff}| < 20\%$ for all locations, from which more than 80% of locations have a $|\text{nDiff}| < 10\%$. These results indicate that annual ideal loads in commercial buildings have low sensitivity to the climatic boundary conditions independently of the performance of the building, which can be because climatic loads are much lower than the internal heat gains.

Given the high internal gains of the commercial buildings, the peak cooling loads become more sensitive than in the residential buildings, see Figs. 19e and f. Note that these cooling peaks are more sensitive in the Target model. This is because the target design has fewer heat losses, which would be "useful" looses to diminish such cooling load peaks.

3.2.3. Influence on BPS results due only to solar radiation models

Whether the configurations of the TMYs would not change due to the use of different solar radiation models, this Section aims to evaluate the uncertainty or the impact that can be reflected on the BPS results due only to the use of different solar radiation modeling approaches. Therefore, the solar radiation data of TMYx.2003–2017 and TMYx.2004–2018 is replaced with the ones obtained by the IWEC2 modeling approach. This means ZHM (see

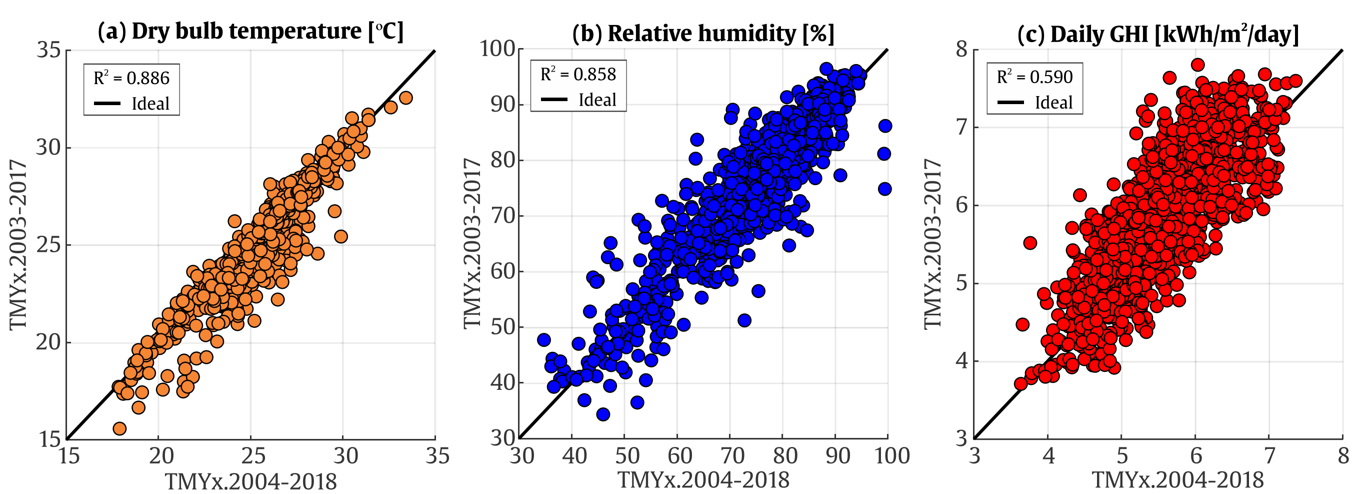

Fig. 15. Correlation between the resulting monthly mean values of the primary variables in the TMYx.2003–2017 and TMYx.2004–2018 databases, which are used to determine the TMYs in ISO 15927–4:2005 method. (a) Monthly mean dry bulb temperature; (b) Monthly mean relative humidity; (c) Monthly mean daily GHI.

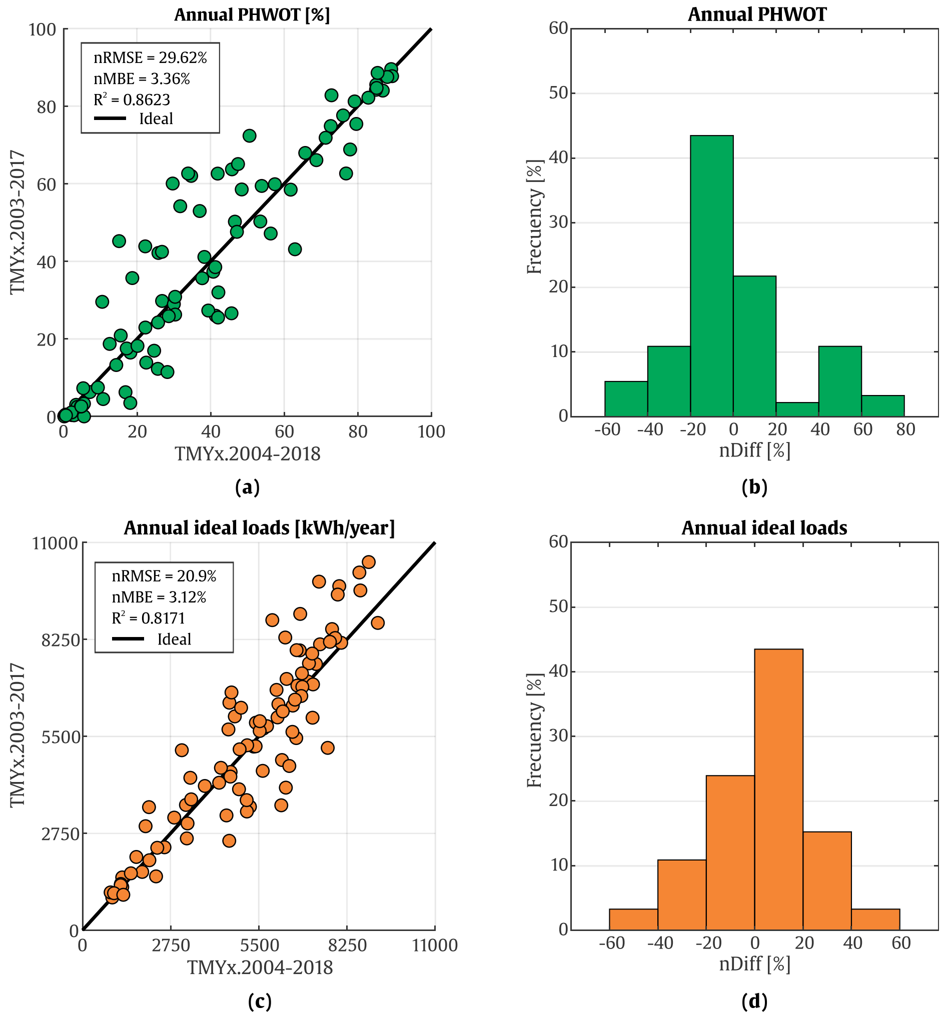

Fig. 16. Comparison of annual BPS results for the target residential building obtained by both databases TMYx.2003–20017 and TMYx.2004–2018 in 92 Brazilian locations.

Eq. (2)) to obtain GHSR and the use of a splitting model based on Gompertz function to obtain the direct normal and diffuse components [62].

So, with these databases, a comparison is performed between the BPS results obtained by the original TMYx databases (TMYx.2003–2017 or TMYx.2004–2018) against the same database with the modified solar radiation and using the same studied buildings within the Brazilian regulations.

Residential buildings Figs. 20a and b show the nDiff obtained for the annual PHWOT index in the target residential building in both database periods (2003–2017 and 2004–2018). For both periods around 70% of locations present a $|\text{nDiff}| < 10\%$. However, the rest of the locations present major nDiff values including a few ones with nDiff $> 40\%$ and which are just due to a change of solar radiation. It is worth remembering that IWEC vs. IWEC2 solar modeling approaches is being compared for the period 2003–2017, and NRSDB vs. IWEC2 for the period 2004–2018.

Regarding annual ideal loads for this case study, a similar pattern to the annual PHWOT is observed in nDiff distribution, but with a general underestimation of annual loads by IWEC2 solar radiation, see Figs. 20c and d. The differences in these results introduced by a change of radiation model can also be significant for some locations, achieving up to nDiff values lower than -40%.

As to peak loads for cooling, similar to the observed before in residential buildings using the different versions of TMYx databases, most of the locations have a $|\text{nDiff}| < 10\%$. However, for this target building, the are few locations with differences lower than -30%.

Fig. 21 depicts the same nDiff distributions but of the reference model of the residential building. Regarding annual PHWOT, in both periods, a large part of locations presents a $|\text{nDiff}| < 10\%$, see Figs. 21a and b. However, in some locations, considerable differences result from the solar radiation change, which attains Diff $> 70\%$ and 40% for the 2003–2017 and 2004–2018 databases, respectively. These noticeable differences indicate that the PHWOT is highly sensitive to climatic boundary conditions in residential buildings, but particularly to solar radiation. Furthermore, in locations with large nDiff, the accuracy of solar modeling can be contradictory between each other because of the regional performance of the models, i.e. overestimated vs. underestimated, which can highlight, even more, the differences in the BPS results for a sensitive building performance index.

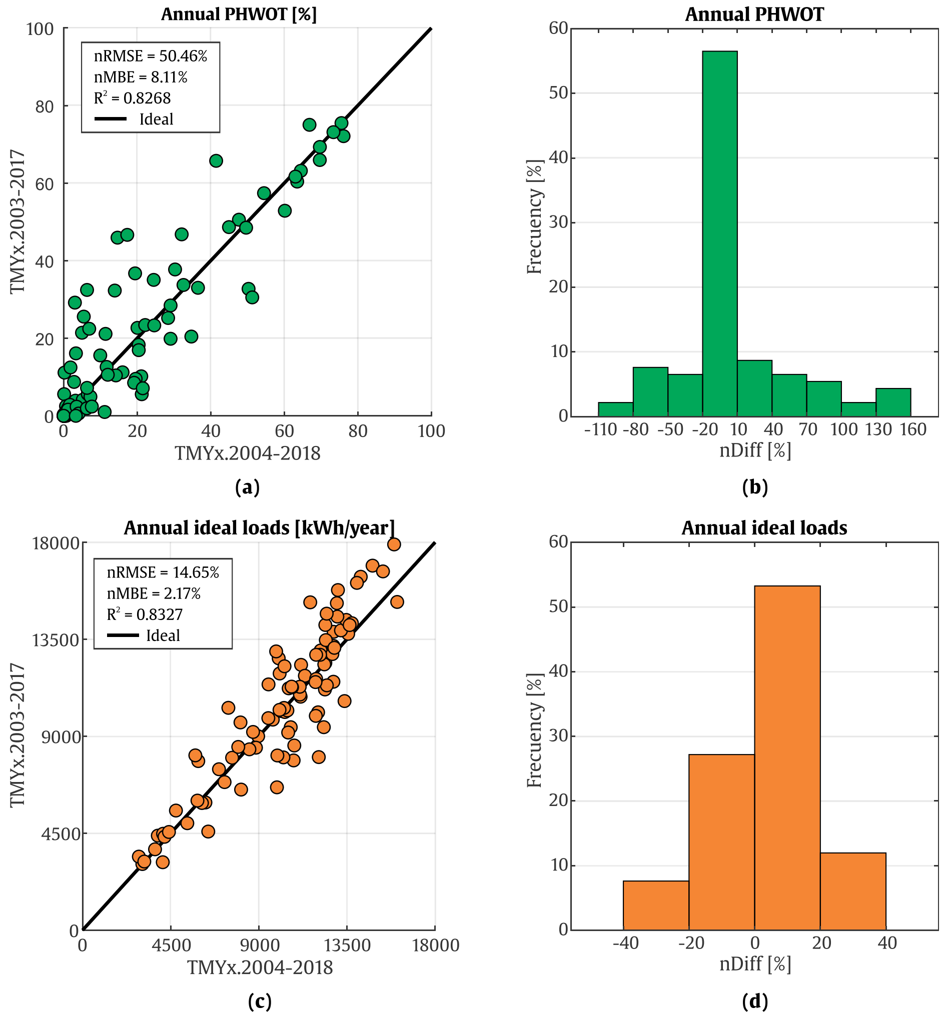

Fig. 17. Comparison of annual BPS results for the reference model of the residential building obtained by both databases TMYx.2003–2017 and TMYx.2004–2018 in 92 Brazilian locations.

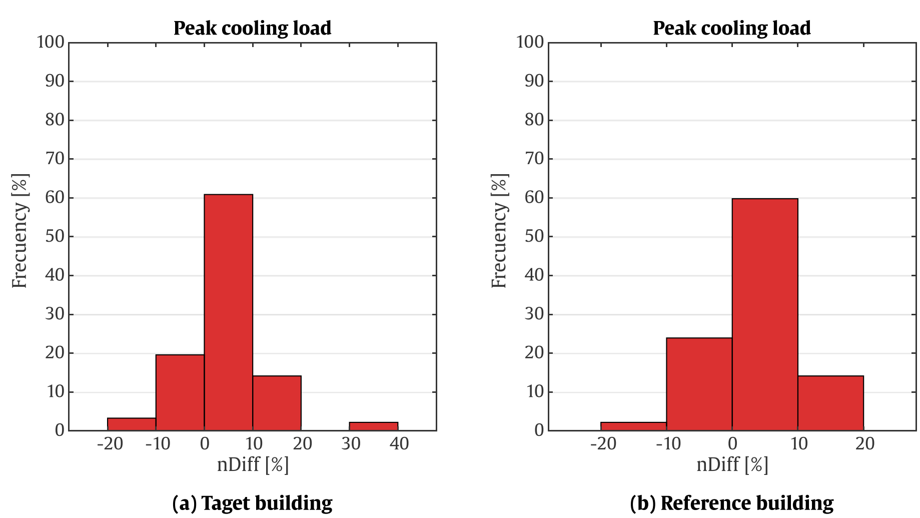

Fig. 18. nDiff of the peak cooling loads for the residential buildings obtained by using both databases, TMYx.2003–2017 and TMYx.2004–2018, in 92 Brazilian locations.

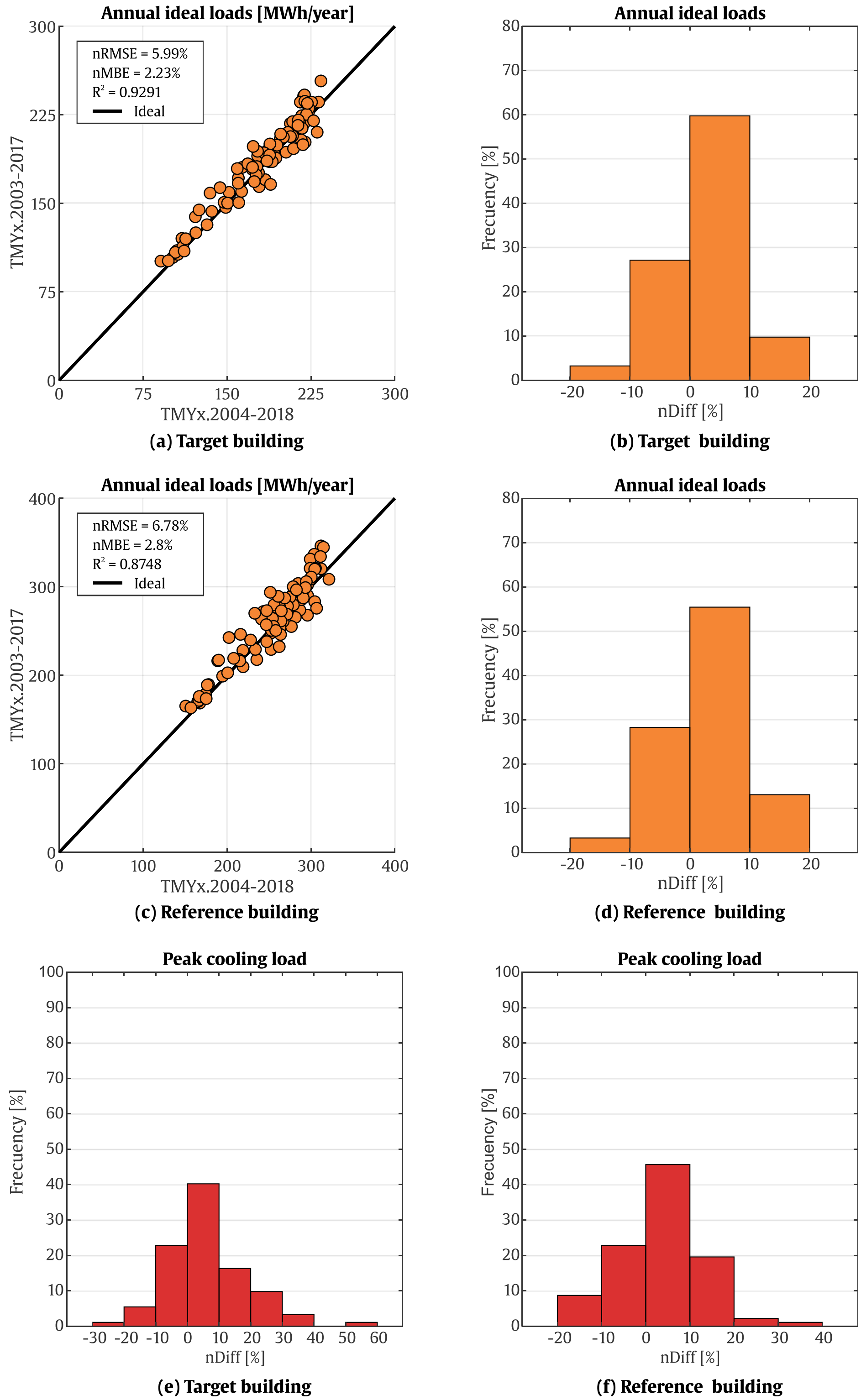

Fig. 19. Comparison of annual ideal loads for the target office building and its reference model obtained by both databases TMYx.2003–2017 and TMYx.2004–2018 in 92 Brazilian locations.

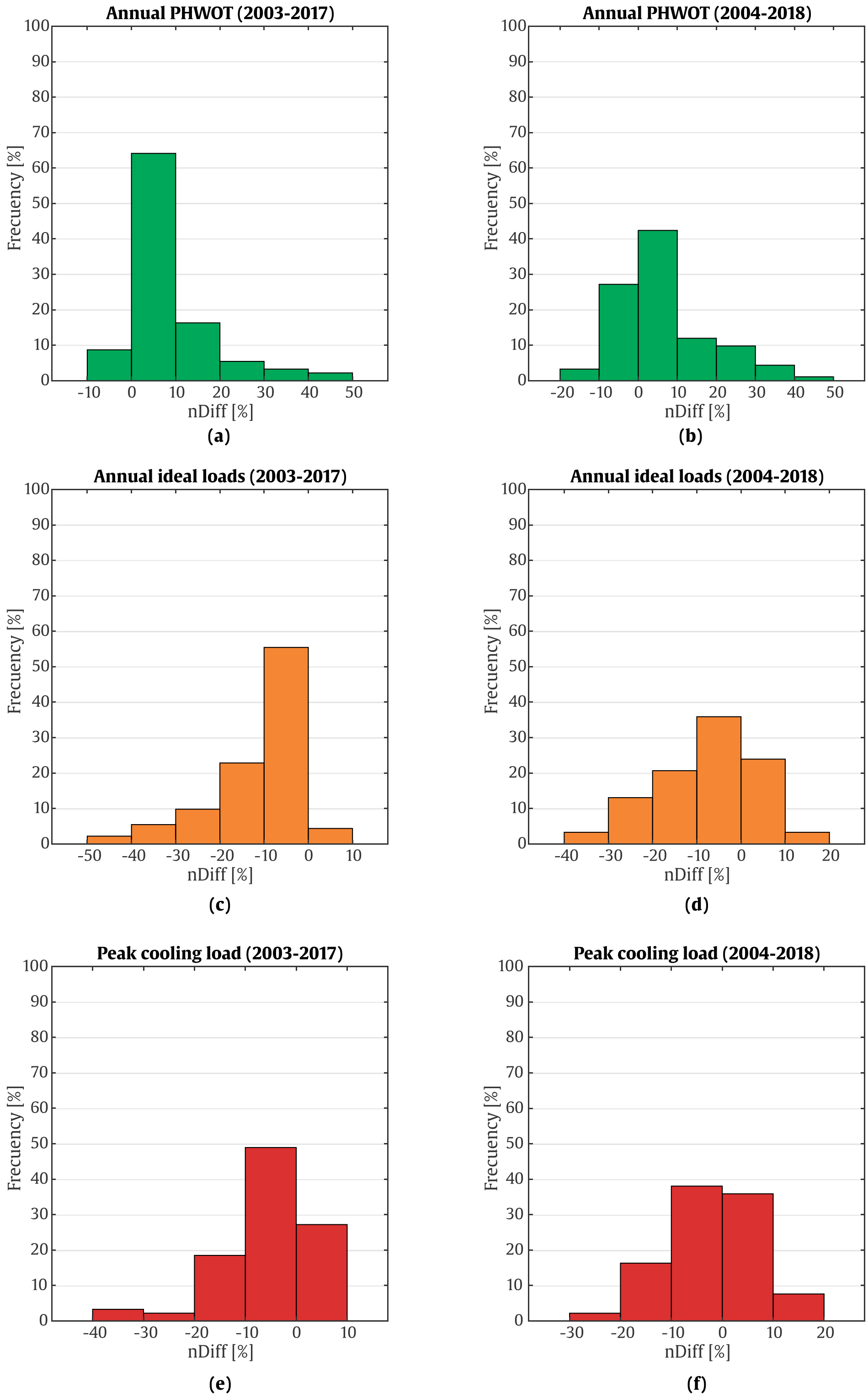

Fig. 20. nDiff distribution of the target residential building driven only by a change of solar radiation modeling in both original databases (TMYx.2003–2017 and TMYx.2004–2018).

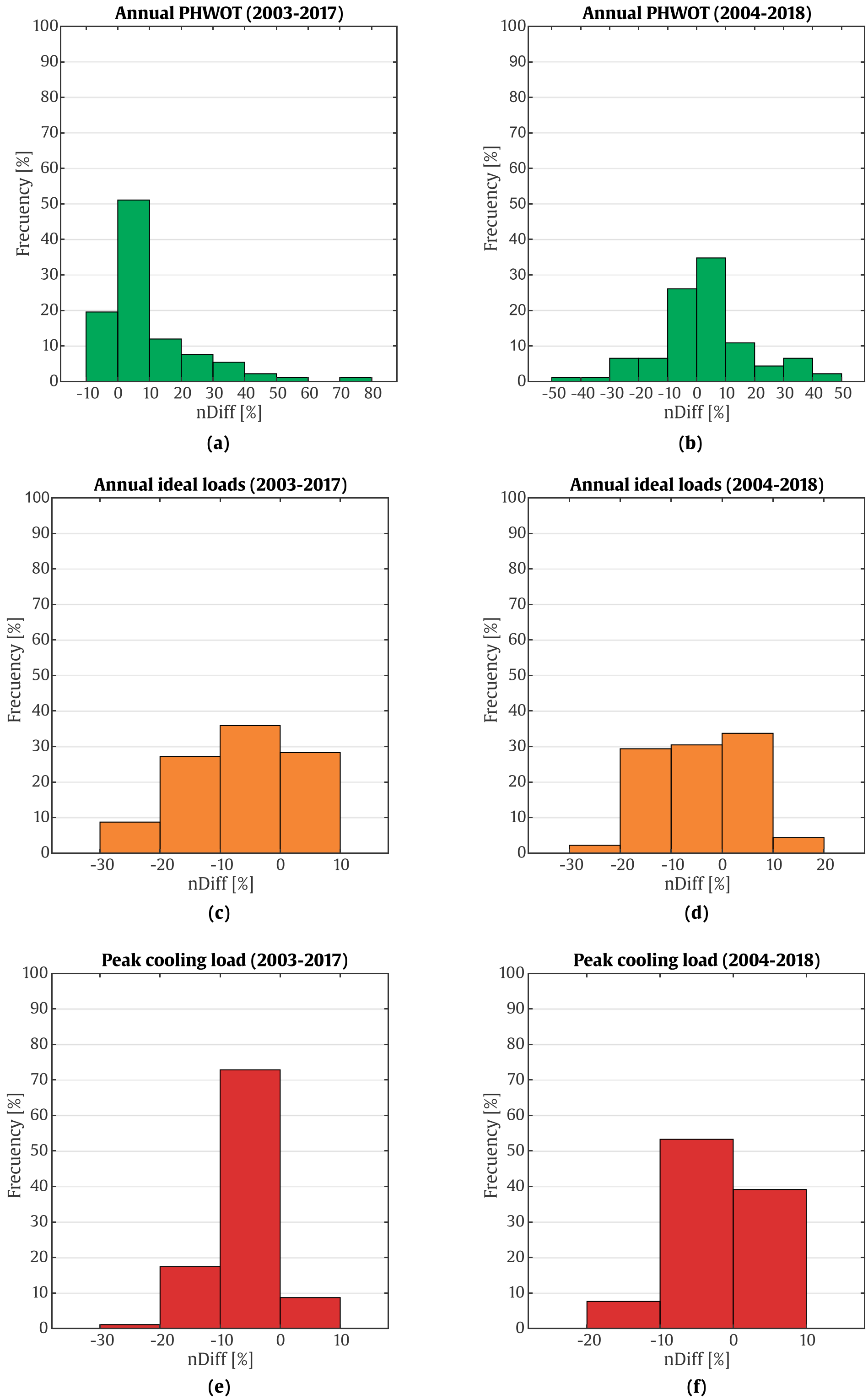

Fig. 21. nDiff distribution of the reference residential building driven only by a change of solar radiation modeling in both original databases (TMYx.2003–2017 and TMYx.2004–2018).

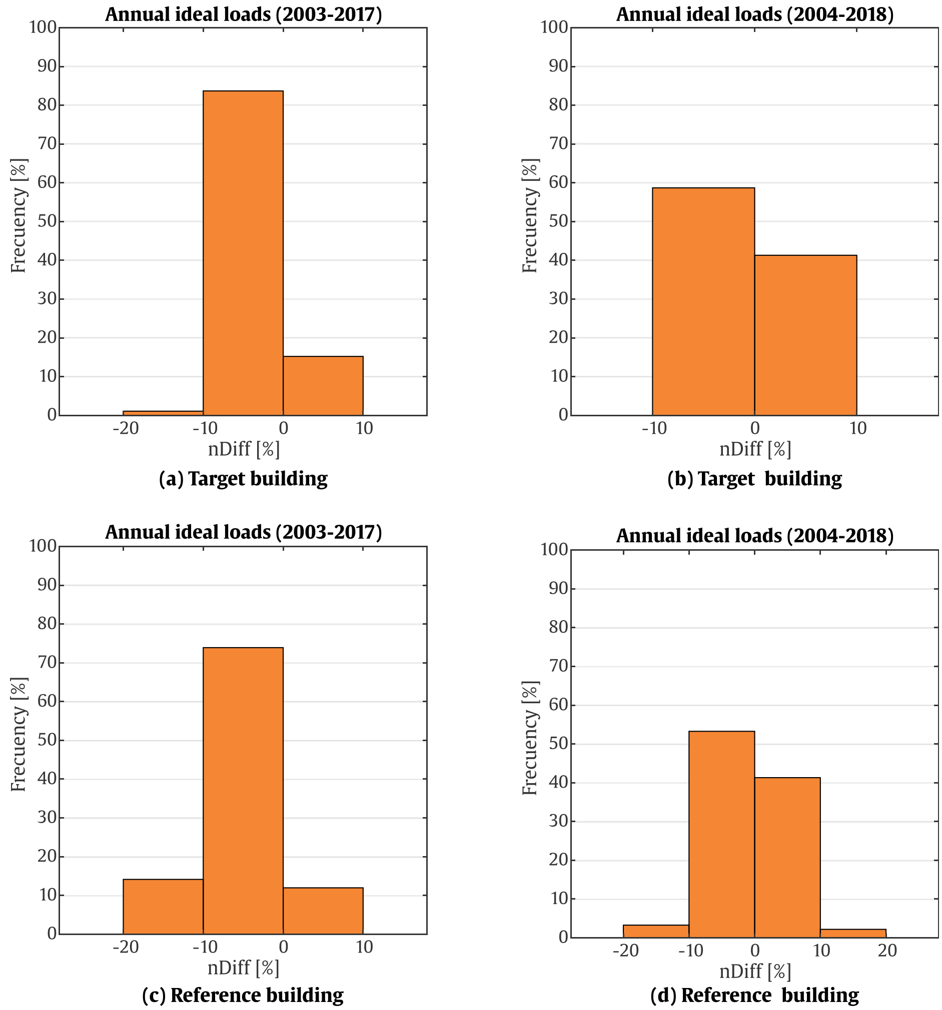

Fig. 22. nDiff distribution of annual ideal loads for the target commercial building and its reference model driven only by a change of solar radiation modeling in both original databases (TMYx.2003–2017 and TMYx.2004–2018).

Differences in annual loads for this reference model are less noticeable than for the target one, this means that the nDiff are less than 20% for more than 90% of locations. The same occurs for peak loads for cooling, where the low insulation of the envelope in the reference case makes it less sensitive than the target one, see Figs. 21e and f.

Commercial buildings Fig. 22 shows the impact of solar radiation modeling on the prediction of annual loads in commercial buildings like the target office and its reference model. Previously we found that annual ideal loads in commercial buildings have low sensitivity to the climatic boundary conditions independently of the performance of the building. Therefore, in these cases that only solar radiation was changed, the differences are also small ($|nDiff| < 10\%$ in most locations). However, the nDiff in these cases are very similar in magnitude and distribution to the driven ones by the changes in the TMY configurations, which indicates that solar radiation is one of the most influential variables on the performance of commercial buildings in Brazil.

Regarding peak loads for cooling, these are less sensitive to the change only of solar radiation data than the TMY configurations. However, the pattern that peak loads for cooling are more sensitive in the target model than in the reference one is still clearly observed, see Fig. 23.

4. Conclusions

A comprehensive study was performed to assess the quality of solar radiation data included in the most recent Typical Meteorological Year (TMY) databases for Brazilian locations and how that quality can influence the selection of months that constitute the TMYs as well as the building performance simulation (BPS) results.

Initially, a previous validation of POWER data was carried out against the global horizontal solar radiation (GHSR) derived from four Baseline stations in Brazil. The results of this validation showed that POWER data is accurate enough to take as standard throughout Brazil. Then, GHSR data of two actual and free available TMYx databases (TMYx.2003–2017 and TMYx.2004–2018) for Brazil were analyzed and compared against the corresponding satellite-derived ones obtained from the POWER database (NASA). Simultaneously, to include the state-of-art on solar radiation modeling for TMY generation, GHSR data are also calculated for the same locations and periods through the IWEC2 approach, and its performance was also compared against the corresponding satellite-derived data.

From this analysis, was observed that the IWEC solar modeling approach, which is employed in all locations of TMYx.2003–2017, presents a low accuracy prediction in most Brazilian locations. This

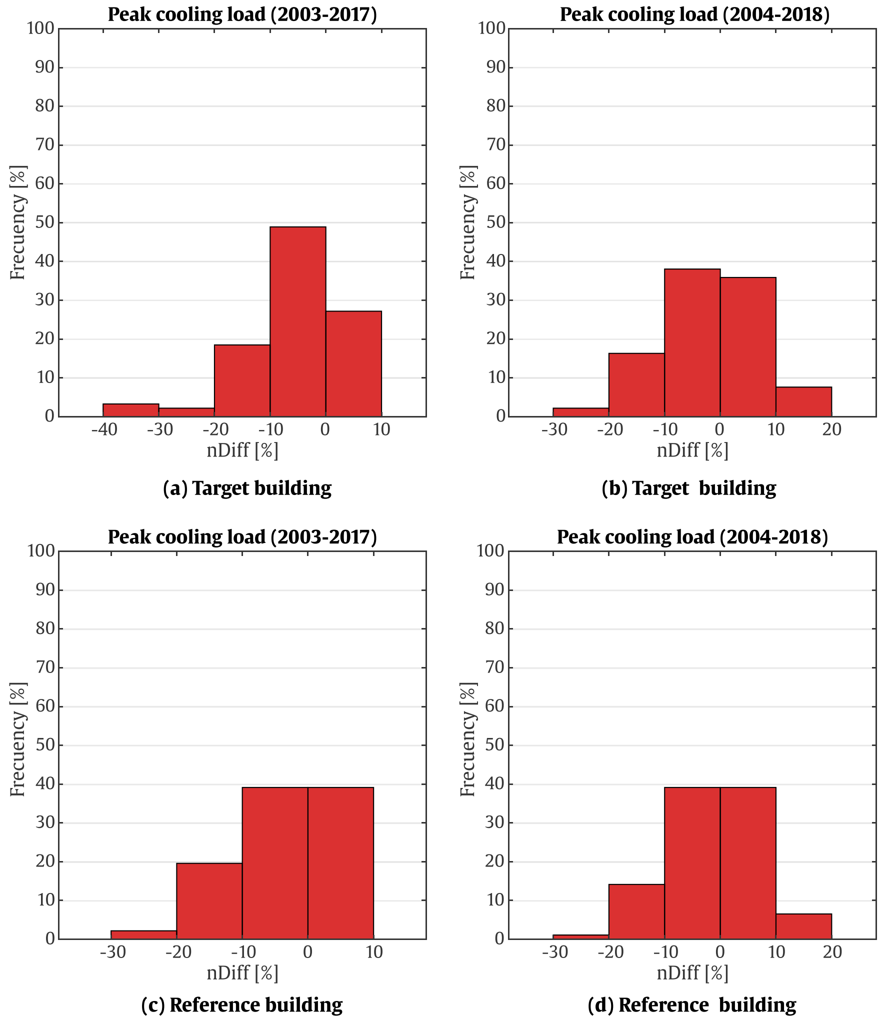

Fig. 23. nDiff distribution of peak loads for cooling in the target commercial building and its reference model driven only by a change of solar radiation modeling in both original databases (TMYx.2003–2017 and TMYx.2004–2018).

was particularly noticeable in tropical locations and during the summer months. Furthermore, GHSR data from NSRDB, which is included in most Brazilian locations in the TMYx.2004–2018 database, considerably improved the accuracy of solar radiation on such locations. On the other hand, the IWEC2 approach showed to be robust and obtained an acceptable accuracy throughout Brazil and for both TMYx database periods.

As another contribution, the impact of solar modeling in the resulting TMY configuration and BPS results was studied. The first conclusion of this part is that the accuracy of the employed solar radiation models can highly influence the selected typical meteorological months that constitute the TMYs. Furthermore, these changes demonstrated that can significantly impact building performance predicted through simulation within the design stage as well as the predicted one within the Brazilian building performance regulations. In particular, the impact was considerably noticeable in residential buildings, in which annual ideal loads presented differences upper 40% and differences upper 130% were found for the percentage of hours within a preset range of operative temperatures (PHWOT). On the other hand, the changes in the TMY configurations did not produce major differences in the prediction of annual loads in commercial buildings, showing absolute differences lower than 10% in most locations and independently of the performance of the analyzed building.

To deeper analyze the impact that can drive solar radiation modeling, two modified TMY databases were generated from both original TMYx databases replacing only the solar radiation data by the calculated using the IWEC2 approach. This analysis allowed us to isolate and quantify only the effect of the accuracy of solar radiation models on the BPS results. Regarding residential case studies, modify only solar radiation in a TMY because the accuracy of models also showed considerable effects for both indicators employed in the Brazilian regulation, that is, annual loads and annual PHWOT. As to commercial buildings, the annual loads resulting from modifying solar radiation did not present great differences, however, those differences have the same order of magnitude as the ones obtained by strong modification of TMY configurations. Therefore, it can be concluded that solar radiation is the most influential climatic variable among the other ones in the performance of commercial buildings.

The impact on the peak loads for cooling was also analyzed for all case studies. The peak loads for cooling demonstrated to be more sensitive in the commercial buildings than in the residential ones regarding climate conditions, which is driven by their large internal gains. Furthermore, the peak loads for cooling are more sensitive in the models with the highest performances (target models). This is driven by their more thermal isolated envelopes and their less capacity to evacuate the peak loads for cooling. These conclusions about the influence of climate conditions on the peak loads are important to take into account during the dimension of the Heating, Ventilation, and Air-Conditioning (HVAC) systems.

Given the main conclusions of this work, it is highly recommended that Brazilian building designers use the last updated TMYx database and keep following the next versions. On the other hand, it is worth noting that the improvement of hourly-resolution solar radiation models is still a big open challenge since an important part of Brazil remains with calculated GHRS and most of the radiation is still modeling and calculated around the globe. In this same line, validating and including the next generation of satellite-derived hourly solar data in TMY files for BPS would be a great contribution.

Data availability

To closer analysis or its reproducibility, the results of the solar radiation data as well as detailed information of all the locations, including latitude, longitude, altitude, and their WMO IDs can be found at https://doi.org/10.17632/hwmm8bsjpd.12. All BPS results are also provided along with the solar radiation data at the same repository.

Declaration of Competing Interest

The authors declare that they have no known competing financial interests or personal relationships that could have appeared to influence the work reported in this paper.

Acknowledgments

For funding this work, we would like to thank the following institutions:

1. National Agency for Scientific and Technological Promotion (ANPCyT), Argentina, via the project PICT-2018-03252 Res. N° 401-19

2. Conselho Nacional de Desenvolvimento Científico e Tecnológico (CNPq), Brazil.

Coordenação de Aperfeiçoamento de Pessoal de Nível Superior (CAPES), Brazil.

Appendix A. Set up of building performance simulations

A.1. Residential buildings

Table A.4.

Table A.4
Details of target and reference models for the residential building analysis.

Model	Details	Target building	Reference building
General configurations	North axis	0	
	Terrain	Suburbs	
	Solar distribution	FullExteriorWithReflections	
	Timestep	6	
Ground modeling	Type	FiniteDifference	
	FiniteDifference: Conductivity	1	
	FiniteDifference: Density	1250	
	FiniteDifference: Specific heat	1200	
	FiniteDifference: Moisture [%]	30	
	FiniteDifference: Moisture at saturation [%]	50	
	FiniteDifference: Evapotranspiration	0.4	
External wall	Thermal resistance [m^2K/W]	1.294	0.057
	Thermal capacity [kJ/m^2K]	30	220
	External solar absorptance [$0-1$]	0.38	0.6
	Internal solar absorptance [$0-1$]	0.6	0.6
Internal wall	Thermal resistance [m^2K/W]	1.321	0.057
	Thermal capacity [kJ/m^2K]	20	220
	External solar absorptance [$0-1$]	0.6	0.6
	Internal solar absorptance [$0-1$]	0.6	0.6
Attic	Roof: Thermal resistance [m^2K/W]	0.0095	0.00923
	Roof: Thermal capacity [kJ/m^2K]	18	11
	Roof: External solar absorptance [$0-1$]	0.35	0.67
	Roof: Internal solar absorptance [$0-1$]	0.35	0.67
	Attic height [m]	1.6	
	Ceiling: Thermal resistance [m^2K/W]	0.087	0.057
	Ceiling: Thermal capacity [kJ/m^2K]	220	220
	Ceiling: External solar absorptance [$0-1$]	0.6	0.6
	Ceiling: External solar absorptance [$0-1$]	0.6	0.6
Floor	Thermal resistance [m^2K/W]	0.054	0.057
	Thermal capacity [kJ/m^2K]	164	220
	External solar absorptance [$0-1$]	0.6	0.6
	Internal solar absorptance [$0-1$]	0.6	0.6
Window	Thermal transmitance [W/m^2K]	2.72	5.7
	Solar heat gain factor [$0-1$]	0.764	0.87
	Glass type	Double	Single
	Window to floor ratio	0.17	
	Frame: Width [m]	0.05	

Table A.4 (*continued*)

Model	Details	Target building	Reference building
	Frame: Projection [m]	0	
	Frame: Conductance [W/m^{2}K]	56	
	Frame: Absorptance	0.58	
	Frame: Emissivity	0.9	
Shutter	Shading control type	OutdoorTemperature	AlwaysOff
	Outdoor air temperature [°C]	26	–
	Slat Orientation [m]	Horizontal	–
	Slat Width [m]	0.05	–
	Slat Separation [m]	0.03	–
	Slat Thickness [m]	0.0042	–
	Slat Angle [–]	45	–
	Slat Conductivity [W/mK]	0.29	–
	Solar Transmittance	0.14	–
	Solar Reflectance	0.04	–
	Blind to Glass Distance [m]	0.05	–
Geometry	Floor to floor height [m]	2.5	
	Total conditioned area of floors [m^2]	38.6	
	Eaves [m]	0.5	–
Internal gains	People number: Living room	4	
	People number: Bedroom	2	
	People: Fraction radiant	0.3	
	People: Living room activities [W]	108	
	People: Bedroom activities [W]	81	
	Lights: Watts per m^2	5	
	Lights: Return Air Fraction	0	
	Lights: Fraction Radiant	0.32	
	Lights: Fraction Visible	0.23	
	Lights: Fraction Replaceable	0	
	Equipments: Watts	120	
	Equipments: Fraction Radiant	0.3	

A.2. Commercial buildings

Table A.5.

Table A.5
Details of target and reference models for the commercial building analysis

Model	Details	Target building	Reference building
General configurations	North axis	0	
	Terrain	City	
	Solar distribution	FullExteriorWithReflections	
	Timestep	6	
Ground modeling	Type	FiniteDifference	
	FiniteDifference: Conductivity	1	
	FiniteDifference: Density	1250	
	FiniteDifference: Specific heat	1200	
	FiniteDifference: Moisture [%]	30	
	FiniteDifference: Moisture at saturation [%]	50	
	FiniteDifference: Evapotranspiration	0.4	
External wall	Thermal resistance [m^{2}K/W]	1.294	0.25
	Thermal capacity [kJ/m^{2}K]	30	151
	External solar absorptance [0 – 1]	0.38	0.5
	Internal solar absorptance [0 – 1]	0.3	0.3
Internal wall	Thermal resistance [m^{2}K/W]	0.277	0.25
	Thermal capacity [kJ/m^{2}K]	167	151
	External solar absorptance [0 – 1]	0.3	0.3
	Internal solar absorptance [0 – 1]	0.3	0.3
Roof	Thermal resistance [m^{2}K/W]	0.306	0.27
	Thermal capacity [kJ/m^{2}K]	238	231
	External solar absorptance [0 – 1]	0.35	0.8
	Internal solar absorptance [0 – 1]	0.3	0.3
Floor	Thermal resistance [m^{2}K/W]	0.123	
	Thermal capacity [kJ/m^{2}K]	160	
	External solar absorptance [0 – 1]	0.3	
	Internal solar absorptance [0 – 1]	0.3	
Internal floor	Thermal resistance [m^{2}K/W]	0.057	

(*continued on next page*)

Table A.5 (*continued*)

<table>
<tr><th>Model</th><th>Details</th><th>Target building</th><th>Reference building</th></tr>
<tr><td></td><td>Thermal capacity [kJ/m^{2}K]</td><td colspan="2">250</td></tr>
<tr><td></td><td>External solar absorptance [0 – 1]</td><td colspan="2">0.3</td></tr>
<tr><td></td><td>Internal solar absorptance [0 – 1]</td><td colspan="2">0.3</td></tr>
<tr><td>Window</td><td>Thermal transmitance [W/m^{2}K]</td><td>2.305</td><td>5.7</td></tr>
<tr><td></td><td>Solar heat gain factor [0 – 1]</td><td>0.185</td><td>0.82</td></tr>
<tr><td></td><td>Glass type</td><td>Double</td><td>Single</td></tr>
<tr><td></td><td>Window to wall ratio</td><td colspan="2">0.5</td></tr>
<tr><td>Shutter</td><td>Shading control type</td><td colspan="2">AlwaysOff</td></tr>
<tr><td>Geometry</td><td>Number of floors</td><td colspan="2">3</td></tr>
<tr><td></td><td>Floor to floor height [m]</td><td colspan="2">3</td></tr>
<tr><td></td><td>Total conditioned area of floors [m^2]</td><td colspan="2">837</td></tr>
<tr><td>Internal gains</td><td>People: Person per m^2</td><td colspan="2">0.1</td></tr>
<tr><td></td><td>People: Fraction radiant</td><td colspan="2">0.3</td></tr>
<tr><td></td><td>People: Activity [W]</td><td colspan="2">120</td></tr>
<tr><td></td><td>Lights: Watts per m^2</td><td colspan="2">14.1</td></tr>
<tr><td></td><td>Lights: Return Air Fraction</td><td colspan="2">0</td></tr>
<tr><td></td><td>Lights: Fraction Radiant</td><td colspan="2">0.32</td></tr>
<tr><td></td><td>Lights: Fraction Visible</td><td colspan="2">0.23</td></tr>
<tr><td></td><td>Lights: Fraction Replaceable</td><td colspan="2">0</td></tr>
<tr><td></td><td>Equipments: Watts per m^2</td><td colspan="2">9.7</td></tr>
<tr><td></td><td>Equipments: Fraction Radiant</td><td colspan="2">0.3</td></tr>
<tr><td>Ventilation</td><td>Type modeling</td><td colspan="2">Infiltration</td></tr>
<tr><td></td><td>Infiltration rate (ACH)</td><td colspan="2">0.3</td></tr>
<tr><td>AC system</td><td>Type</td><td colspan="2">Ideals loads</td></tr>
<tr><td></td><td>Heating setpoint [°C]</td><td colspan="2">18</td></tr>
<tr><td></td><td>Cooling setpoint [°C]</td><td colspan="2">24</td></tr>
<tr><td></td><td>Dehumidification</td><td colspan="2">No</td></tr>
<tr><td></td><td>Outdoor Air Flow Rate per Person (m^3/s)</td><td colspan="2">0.0075</td></tr>
</table>

References

[1] International Hydropower Association, et al., Hydropower status report: Sector trends and insights, in: International Hydropower Association, London, UK, 2018.
[2] Viviane de Souza Dias, Marta Pereira da Luz, Gabriela M Medero, and Diego Tarley Ferreira Nascimento, An overview of hydropower reservoirs in brazil: Current situation, future perspectives and impacts of climate change, Water 10 (5) (2018) 592.
[3] Luiz Pinguelli Rosa, Louise Land B. Lomardo, The brazilian energy crisis and a study to support building efficiency legislation, Energy Build. 36(2) (2004) 89–95. doi:10.1016/j.enbuild.2003.09.001.
[4] ABNT NBR 15220-3: Desempenho térmico de edificações – Parte 3: Zoneamento bioclimático brasileiro e diretrizes construtivas para habitações unifamiliares de interesse social. ASSOCIAÇÃO BRASILEIRA DE NORMAS TÉCNICAS, Rio de Janeiro, RJ, Brazil, 2005.
[5] ABNT NBR 15575: Edifícios habitacionais – Desempenho. ASSOCIAÇÃO BRASILEIRA DE NORMAS TÉCNICAS, Rio de Janeiro, RJ, Brazil, 2008.
[6] Ing Liang Wong, Eduardo Krüger, Comparing energy efficiency labelling systems in the EU and brazil: implications, challenges, barriers and opportunities, Energy Policy 109 (2017) 310–323, https://doi.org/10.1016/j.enpol.2017.07.005.
[7] G. Calleja Rodríguez, A. Carrillo Andrés, F. Domínguez Muñoz, J.M. Cejudo López, Y. Zhang, Uncertainties and sensitivity analysis in building energy simulation using macroparameters, Energy Build. 67 (2013) 79–87. ISSN 0378–7788. doi:10.1016/j.enbuild.2013.08.009.
[8] Daniel Coakley, Paul Raftery, Marcus Keane, A review of methods to match building energy simulation models to measured data, Renew. Sustain. Energy Rev. 37 (2014) 123–141. ISSN 1364–0321. doi:10.1016/j.rser.2014.05.007.
[9] Leonardo Mazzaferro, Rayner M.S. Machado, Ana Paula Melo, Roberto Lamberts, Do we need building performance data to propose a climatic zoning for building energy efficiency regulations? Energy Build. 225 (2020) 110303. ISSN 0378–7788. doi:10.1016/j.enbuild.2020.110303.
[10] Ying Cui, Da Yan, Tianzhen Hong, Chan Xiao, Xuan Luo, Qi Zhang, Comparison of typical year and multiyear building simulations using a 55-year actual weather data set from china, Appl. Energy 195 (2017) 890–904. ISSN 0306–2619. doi:10.1016/j.apenergy.2017.03.113.
[11] Gianpiero Evola, Vincenzo Costanzo, Marco Infantone, Luigi Marletta, Typical-year and multi-year building energy simulation approaches: a critical comparison, Energy 219 (2021) 119591. ISSN 0360–5442. doi:10.1016/j.energy.2020.119591.
[12] National Climatic Center (NCC), Test Reference Year (TRY), DSI-9706 (1976).
[13] I.J. Hall, R.R. Prairie, H.E. Anderson, E.C. Boes, Generation of typical meteorological years for 26 SOLMET stations (Technical Report SAND 78–1601), Sandia National Laboratories, Albuquerque, New Mexico, USA, 1978.
[14] ISO 15927-4:2005, Hygrothermal performance of buildings – Calculation and presentation of climatic data - Part 4: Hourly data for assessing the annual energy use for heating and cooling, International Organization for Standardization (2005).
[15] W. Marion, K. Urban, User's Manual for TMY2s Typical Meteorological Years, National Renewable Energy Laboratory, U.S. Department of Energy, Golden, CO, USA, 1995.
[16] S. Wilcox, W. Marion, Users Manual for TMY3 Data Sets (Technical Report NREL/TP-581-43156), National Renewable Energy Laboratory, U.S. Department of Energy, Golden, CO, USA, 2008.
[17] Loren W. Crow, Weather year for energy calculations, ASHRAE J. (United States) 26 (1984).
[18] D. Thevenard, A. Brunger, Typical weather years for international locations, ASHRAE Research Project (2001).
[19] Y.J. Huang, F. Su, D. Seo, M. Krarti, Development of 3012 IWEC2 weather files for international locations (RP-1477), ASHRAE Trans. 120(Part 1) (2014) 340–355.
[20] O.S. Ohunakin, M.S. Adaramola, O.M. Oyewola, R.O. Fagbenle, Generation of a typical meteorological year for north–east, Nigeria, Appl. Energy 112 (2013) 152–159.
[21] K. Skeiker, Generation of a typical meteorological year for Damascus zone using the Filkenstein-Schafer statistical method, Energy Convers. Manage. 45 (2004) 99–112.
[22] S. Janjai, P. Deeyai, Comparison of methods for generating typical meteorological year using meteorological data from a tropical environment, Appl. Energy 86 (2009) 528–537.
[23] Y. Jiang, Generation of typical meteorological year for different climates of China, Energy 35 (2010) 1946–1953.
[24] S. Pusat, İ. Ekmekçi, M.T. Akkoyunlu, Generation of typical meteorological year for different climates of Turkey, Renew. Energy 75 (2015) 144–151.
[25] F. Bre, V.D. Fachinotti, Generation of typical meteorological years for the argentine littoral region, Energy Build. 129 (2016) 432–444. ISSN 0378–7788. doi:10.1016/j.enbuild.2016.08.006.
[26] D.B. Crawley, Which weather data should you use for energy simulations of commercial buildings?, Trans-Am. Soc. Heat. Refrig. Air Condition. Eng. 104 (1998) 498–515.
[27] D.B. Crawley, C.S. Barnaby, Weather and climate in building performance simulation, in: Building Performance Simulation for Design and Operation, Routledge, 2019, pp. 191–220.
[28] A. Moazami, V.M. Nik, S. Carlucci, S. Geving, Impacts of future weather data typology on building energy performance – investigating long-term patterns

of climate change and extreme weather conditions, Appl. Energy 238 (2019) 696–720. ISSN 0306–2619. doi:10.1016/j.apenergy.2019.01.085.
[29] A. Moazami, S. Carlucci, V.M. Nik, S. Geving, Towards climate robust buildings: an innovative method for designing buildings with robust energy performance under climate change, Energy Build. 202 (2019) 109378. ISSN 0378–7788. doi:10.1016/j.enbuild.2019.109378.
[30] M.A.D. Larsen, S. Petrović, A.M. Radoszynski, R. McKenna, O. Balyk, Climate change impacts on trends and extremes in future heating and cooling demands over europe, Energy Build. 226 (2020) 110397. ISSN 0378–7788. doi:10.1016/j.enbuild.2020.110397.
[31] T.-T. Chow, A.L.S. Chan, K.F. Fong, Z. Lin, Some perceptions on typical weather year–from the observations of hong kong and macau, Sol. Energy 80 (4) (2006) 459–467.
[32] S. Erba, F. Causone, R. Armani, The effect of weather datasets on building energy simulation outputs, Energy Proc. 134 (2017) 545–554.
[33] J. Zhang, L. Zhao, S. Deng, W. Xu, Y. Zhang, A critical review of the models used to estimate solar radiation, Renew. Sustain. Energy Rev. 70 (2017) 314–329.
[34] E.L. Maxwell, Metstat–the solar radiation model used in the production of the national solar radiation data base (nsrdb), Sol. Energy 62 (4) (1998) 263–279.
[35] F. Kasten, G. Czeplak, Solar and terrestrial radiation dependent on the amount and type of cloud, Solar Energy 24 (2) (1980) 177–189.
[36] Q. Zhang, J. Huang, S. Lang, Development of typical year weather data for Chinese locations, ASHRAE Trans. 108(Pt. 2) (2002).
[37] Q. Zhang, Development of the typical meteorological database for Chinese locations, Energy Build. 38 (2006) 1320–1326.
[38] K.H. Kim, J.K.-W. Oh, W. Jeong, Study on solar radiation models in south korea for improving office building energy performance analysis, Sustainability 8 (6) (2016) 589.
[39] H.D. Kambezidis, B.E. Psiloglou, The meteorological radiation model (mrm): advancements and applications, in: Modeling solar radiation at the earth's surface, Springer, 2008, pp. 357–392.
[40] K. Yaman, G. Arslan, The impact of hourly solar radiation model on building energy analysis in different climatic regions of turkey, in: Building Simulation, vol. 11, Springer, 2018, pp. 483–495.
[41] J.C. Carlo, R. Lamberts, Processamento de arquivos climáticos para simulação do desempenho energético de edificações, Arquivos Climáticos. Florianópolis: UFSC/LabEEE, 2005.
[42] M. Roriz. Arquivos Climáticos de Municípios Brasileiros, Associação Nacional de Tecnologia do Ambiente Construído (ANTAC), Grupo de Trabalho sobre Conforto e Eficiência Energética de Edificações, 2012. URL: http://www.roriz.eng.br/epw/textunderscore9.html.
[43] D.B. Crawley, L.K. Lawrie, Climate. OneBuilding.Org, 2020. URL: http://climate.onebuilding.org. Accessed June, 2020.
[44] Telma de Oliveira Pitta, Estudo de métodos diretos e indiretos de estimativa de irradiação solar global diária horizontal a partir de observações superficiais de cobertura total de nuvens em florianópolis, sc. 2001.
[45] A. Smith, N. Lott, R. Vose, The integrated surface database: recent developments and partnerships, Bull. Am. Meteorol. Soc. 92 (6) (2011) 704–708.
[46] R. Perez, P. Ineichen, K. Moore, E.L. Maxwell, R.D. Seals, A. Zelenka, Dynamic global-to-direct irradiance conversion models, ASHRAE Trans. 98(Part 1) (2012) 354–369.
[47] M. Sengupta, Y. Xie, A. Lopez, A. Habte, G. Maclaurin, J. Shelby, The National Solar Radiation Data Base (NSRDB), Renew. Sustain. Energy Rev. 89 (2018) 51–60. ISSN 1364–0321. doi:10.1016/j.rser.2018.03.003.
[48] Y. Xie, M. Sengupta, J. Dudhia, A Fast All-sky Radiation Model for Solar applications (FARMS): Algorithm and performance evaluation, Solar Energy 135 (2016) 435–445. ISSN 0038–092X. doi:10.1016/j.solener.2016.06.003.
[49] Taiping Zhang, William S. Chandler, James M. Hoell, David Westberg, Charles H. Whitlock, Paul W. Stackhouse, A Global Perspective on Renewable Energy Resources: Nasa's Prediction of Worldwide Energy Resources (POWER) Project. In Proceedings of ISES World Congress 2007 (Vol. I–Vol. V), pages 2636–2640. Springer, 2008. URL: https://power.larc.nasa.gov/.
[50] Jinshun Bai, Xinping Chen, Achim Dobermann, Haishun Yang, Kenneth G. Cassman, Fusuo Zhang, Evaluation of nasa satellite-and model-derived weather data for simulation of maize yield potential in china, Agron. J. 102 (1) (2010) 9–16.
[51] Jeffrey W. White, Gerrit Hoogenboom, Paul W. Wilkens, Paul W. Stackhouse Jr, James M. Hoel, Evaluation of satellite-based, modeled-derived daily solar radiation data for the continental united states, Agron. J. 103 (4) (2011) 1242–1251.
[52] Germán Salazar, Christian Gueymard, Janis Bezerra Galdino, Olga de Castro Vilela, Naum Fraidenraich, Solar irradiance time series derived from high-quality measurements, satellite-based models, and reanalyses at a near-equatorial site in brazil, Renew. Sustain. Energy Rev. 117 (2020) 109478.
[53] Amelie Driemel, John Augustine, Klaus Behrens, Sergio Colle, Christopher Cox, Emilio Cuevas-Agulló, Fred M Denn, Thierry Duprat, Masato Fukuda, Hannes Grobe, et al., Baseline surface radiation network (bsrn): structure and data description (1992–2017), Earth Syst. Sci. Data 10(3) (2018) 1491–1501.
[54] E.B. Pereira, Basic measurements of radiation at station Brasilia. Instituto Nacional de Pesquisas Espaciais, Brasilia, PANGAEA, 2008. Accessed: 2021-04-01.
[55] S. Colle, Basic measurements of radiation at station Florianópolis. Universidade Federal de Santa Catarina, PANGAEA, 2007. Accessed: 2021-04-01..
[56] E.B. Pereira, Basic measurements of radiation at station Petrolina. Instituto Nacional de Pesquisas Espaciais, Brasilia, PANGAEA, 2008. Accessed: 2021-04-01.
[57] E.B. Pereira, Basic measurements of radiation at station São Martinho da Serra. Instituto Nacional de Pesquisas Espaciais, Brasilia, PANGAEA, 2008. Accessed: 2021-04-01.
[58] NBR 15575: Desempenho de edificações habitacionais (Performance of residential buildings). ABNT – ASSOCIAÇÃO BRASILEIRA DE NORMAS TÉCNICAS (Brazilian Association of Technical Standards), Rio de Janeiro, RJ, Brazil, 2021.
[59] A cloud-based platform to predict wind pressure coefficients on buildings. Under review. URL: https://cpsimulator.cimec.org.ar/.
[60] Instrução Normativa Inmetro para a Classificação de Eficiência Energética de Edificações Comerciais, de Serviços e Públicas (Inmetro Normative Instruction for the Classification of Energy Efficiency of Commercial, Services and Public Buildings). INMETRO - Instituto Nacional de Metrologia, Qualidade e Tecnologia (National Institute of Metrology, Quality and Technology), Brazil, 2021.
[61] Vincenzo Costanzo, Gianpiero Evola, Marco Infantone, Luigi Marletta, Updated typical weather years for the energy simulation of buildings in mediterranean climate. A case study for sicily, Energies 13 (16) (2020) 4115.
[62] Q.Y. Zhang, C.Z. Lou, H.X. Yang, A new method to separate horizontal solar radiation into direct and diffuse components, Proc. ISESAP 2004 (2004) 682–688.